

Efficient Trajectory Compression and Queries

Hongbo Yin
Harbin Institute of Technology
Harbin, China
hongboyin@hit.edu.cn

ABSTRACT

There are ubiquitousness of GPS sensors in smart-phones, vehicles and wearable devices which have enabled the collection of massive volumes of trajectory data from tracing moving objects. Analyzing on trajectory databases dose benefit many real-world applications, such as route planning and transportation optimizations. However, an unprecedented scale of GPS data has posed an urgent demand for not only an effective storage but also an efficient query mechanism for trajectory databases. So trajectory compression (also called trajectory sampling) is a must, but the existing online compression algorithms either take a too long time to compress a trajectory, need too much space in the worst cases or the difference between the compressed trajectory and the raw trajectory is too big. In response to this question, ϵ -Region based Online trajectory Compression with Error bounded (ROCE for short), whose time and space complexity is $O(N)$ and $O(1)$, is proposed in this paper, which achieves a good balance between the execution time and the difference. As a new error-based quality metric, Point-to-segment Euclidean Distance (PSED for short) is the first proposed by this paper and adopted by ROCE. After the compression, one raw trajectory has been compressed into multiple continuous line segments, not discrete trajectory points any more. As far as we know, we are the first to notice this and make good use of properties of line segments to answer top- k trajectory similarity queries and range queries on the compressed trajectories. We also define a new error-based quality metric Area sandwiched by the Line segments of trajectories (AL) using the area sandwiched by pairs of line segments to describe how two compressed trajectories are similar. We introduces a special index, Balanced spatial Partition quadtree index with data Adaptability (BPA), which can accelerate both trajectory range queries and the top- k trajectory similarity queries with only one same index.

PVLDB Reference Format:

Hongbo Yin. Efficient Trajectory Compression and Queries. PVLDB, 14(1): XXX-XXX, 2020.
doi:XX.XX/XXX.XX

1 INTRODUCTION

The last decade has witnessed an unprecedented growth of mobile devices, such as smart-phones, vehicles, and wearable smart devices. Nearly all of them are equipped with the location-tracking function

and have been widely used to collect massive raw trajectory data of moving objects at a certain sampling rate (e.g. 5 seconds) for location based services, trajectory mining, wildlife tracking and many other useful and meaningful applications. However, the raw trajectory data collected is often very large, and in many application scenarios, it's unacceptable to store and query on the raw trajectories. For example, Fitbit, which is one of the most popular wearable device manufacturing companies for fitness monitor and activity tracker, has 28 million active users up to November 1st, 2019¹. If each wearable device records its latest position every 5 seconds, over 20 billion raw trajectory points in total will be generated just in one hour. It consumes too much network bandwidth, storage space and computing resources to transmit, store and query on such data.

Trajectory compression is a suitable and effective solution to solve the problem. Line simplification is a mainstream compression method and has drawn wide attention, which compresses each raw trajectory into a set of continuous line segments. It's a kind of lossy compression, where a high compression rate can be obtained with a tolerable error bound. Existing line simplification methods fall into two categories, i.e. batch mode and online mode. For each raw trajectory, algorithms in batch mode require that all points of this trajectory must be loaded in the local buffer before compression, which means that the local buffer must be large enough to hold the entire trajectory. Thus, the space complexities of these algorithms are at least $O(N)$, or even $O(N^2)$, which limits the application of these algorithms in resource-constrained environments. Therefore, more work focuses on the other kind of compression methods, algorithms in online mode, which only need a limited size of local buffer, rather than a very lager local buffer to compress trajectories in an online processing manner. Thus algorithms in online mode have much more application scenarios compared with those in batch mode, i.e. compressing streaming data. The existing algorithms all try to reach a good balance among the accuracy loss, the time cost and the compression rate, but the effect is not very ideal. Zhang et al.[36] has conducted experiments on comparing the compression time and the accuracy loss of state-of-the-art algorithms in online mode, and part of the results are shown in Table 1. As the table shows, they either consume too much time if the accuracy loss is small, such as BQS and FBQS, or lose a large number of accuracy if the time cost is acceptable, such as Angular, Interval and OPERB. It's still a big challenge for the existing compression algorithms to compress trajectories into much smaller forms with less time and less accuracy loss. To address this, we propose a new online line simplification compression method ROCE, which makes a perfect balance among the accuracy loss, the time cost and the compression rate. When the compression rate is fixed, with only $O(N)$ time complexity and $O(1)$ space complexity, ROCE is one of the fastest

This work is licensed under the Creative Commons BY-NC-ND 4.0 International License. Visit <https://creativecommons.org/licenses/by-nc-nd/4.0/> to view a copy of this license. For any use beyond those covered by this license, obtain permission by emailing info@vldb.org. Copyright is held by the owner/author(s). Publication rights licensed to the VLDB Endowment.

Proceedings of the VLDB Endowment, Vol. 14, No. 1 ISSN 2150-8097.
doi:XX.XX/XXX.XX

¹<https://expandedramblings.com/index.php/fitbit-statistics/>

algorithms, and its accuracy loss is also the smallest in the fastest algorithms. Such good properties make ROCE have a vast range of applications. For example, it is able to compress streaming data, be run sustainably on resource-constrained devices, and be used to track locations of small animals over a long period of time.

Table 1: The time cost and accuracy loss of some state-of-the-art algorithms in online mode. The compression rates are all fixed at 10.

Algorithm in Online Mode	BQS	FBQS	Angular	Interval	OPERR
Compression Time per Trajectory Point (μ s)	500.91	405.38	0.2	0.28	0.97
The Maximum PED Error	38.23	36.63	1532.65	1889.81	306.2

The purpose of compressing trajectories is to reduce the cost of transmission and storage, especially the computing cost of queries. So, how to execute queries on compressed trajectories is very important. Range queries and top- k similarity queries are two kinds of most fundamental queries for various applications in trajectory data analysis. Some processing methods for these two queries have been proposed. But as far as we know, there is no related work on discussing how to process these two kinds of queries specially on the compressed trajectories which are compressed by line simplification compression methods. Most previous work thinks a trajectory overlaps the query region R iff at least one point of this trajectory is in R . However, this definition is especially not applicable to the situation where the queried trajectories are compressed trajectories consisting of multiple continuous line segments with different lengths. Each trajectory line segment may represent hundreds of raw trajectory points and be dozens of kilometers. There are always such situations where the raw trajectory goes through the query region, but no endpoints of compressed line segments fall in the the query region. To solve problems like this, we propose two algorithms about how to process range queries and top- k trajectory similarity queries based on line segments directly on the compressed trajectories compressed by any line simplification compression method, including ROCE. This is the first work to discuss how to process trajectory queries on compressed trajectories consisting of multiple continuous line segments as far as we know, and the actual effect is quite satisfactory.

The main contributions of this paper are summarized as follows:

- We propose a new online line simplification compression algorithm ROCE with error bounded. It achieves a good balance among the accuracy loss, the time cost and the compression rate. The time and space complexity of ROCE are only $O(N)$ and $O(1)$ respectively. Point-to-Segment Euclidean Distance (PSED), an error criterion, is proposed to measure the deviation of every point and its corresponding line segment after the compression.
- To solve the problem that the old definitions of trajectory queries are no longer suitable for the compressed trajectories, we propose a new range query processing algorithm and a new top- k similarity query processing algorithm based on line segments. These two algorithms can be applied directly on compressed trajectories compressed by any line simplification compression method. This is the first work to discuss how to process trajectory queries on compressed

trajectories consisting of multiple continuous line segments as far as we know.

- To describe the similarity between two compressed trajectories, we define a new error-based quality metric AL based on the area sandwiched by line segments of two trajectories.
- An efficient balanced index BPA and a set of novel techniques are also presented to accelerate the processing of range queries and top- k similarity queries obviously.
- We conduct extensive experiments on real trajectory datasets. The results demonstrate superior performance of our approach on !!!!!!!!!!!!!!!.

The rest of this paper is organized as follows. Section 2 presents basic concepts and definitions. Section 3 introduces a new compression algorithm ROCE. Section 4 introduces an efficient index BPA and the range query algorithm on compressed trajectories. Section 5 gives a new error-based quality metric AL and the top- k similarity query algorithm based on AL. Section 6 shows the sufficient experimental results and analysis. Section 7 reviews related works and finally Section 8 concludes our work.

2 PRELIMINARIES

Definition 2.1. (Trajectory Point): A trajectory point can be seen as a triple $p_i(x_i, y_i, t_i)$, where x_i and y_i represent the coordinate of the moving object at time t_i .

Definition 2.2. (Trajectory): A trajectory $T = \{p_1, p_2, \dots, p_N\}$ is a sequence of trajectory points in a monotonically increasing order of their associated time values (i.e., $t_1 < t_2 < \dots < t_N$). $T[i] = p_i$ is the i th trajectory point in T .

We simplify the representation of each trajectory point p_i into a 2-dimensional subvector (x_i, y_i) because we only care about the order of these trajectory points and we don't care about the exact time when the tracked object is located at (x_i, y_i) .

Given a raw trajectory $T = \{p_1, p_2, \dots, p_N\}$, $T[i : i + m] = \{p_i, p_{i+1}, \dots, p_{i+m}\}$ ($i, m \in N^*$ and $2 \leq i + m \leq N$) is called a trajectory segment of T . Given a trajectory segment $T[i : i + m]$, a line segment $p_i p_{i+m}$, starting from p_i and ending at p_{i+m} , is used to approximately represent $T[i : i + m]$, i.e. $p_i p_{i+m}$ is the compressed form of $T[i : i + m]$. $p_{i+1}, p_{i+2}, \dots, p_{i+m-1}$ are the discarded points, and the corresponding line segments of $p_i, p_{i+1}, \dots, p_{i+m}$ are all $p_i p_{i+m}$. Each raw trajectory can be represented as different sets of consecutive trajectory segments. For example, $T = \{p_1, p_2, \dots, p_{10}\}$ can be represented as $\{T[1 : 5], T[5 : 10]\}$ or $\{T[1 : 4], T[4 : 7], T[7 : 10]\}$.

Definition 2.3. (Compressed Trajectory): Given a raw trajectory $T = \{p_1, p_2, \dots, p_N\}$ and a set of T 's corresponding consecutive trajectory segments, the corresponding compressed trajectory T' of T is a set of consecutive line segments of all trajectory segments in T . T' can be denoted as $\{p_{i_1} p_{i_2}, p_{i_2} p_{i_3}, \dots, p_{i_{n-1}} p_{i_n}\}$ ($p_{i_1} = p_1, p_{i_n} = p_N$).

In order to save space, we can also simplify the form of T' into $\{p_{i_1}, p_{i_2}, \dots, p_{i_n}\}$ ($p_{i_1} = p_1, p_{i_n} = p_N$) to represent $n - 1$ consecutive line segments.

Definition 2.4. (Compression Rate): Given a raw trajectory $T = \{p_1, p_2, \dots, p_N\}$ with N trajectory points and one of its compressed

trajectories, $T' = \{p_{i_1}, p_{i_2}, \dots, p_{i_n}\} (p_{i_1} = p_1, p_{i_n} = p_N)$ with $n - 1$ consecutive line segments, the compression rate is

$$r = N/n.$$

3 ROCE COMPRESSION ALGORITHM

In this section, we first give the detailed description of a new error-based quality metric PSED. And then, we introduce ϵ -Region based Online trajectory Compression with Error bounded (ROCE for short), whose error-based quality metric is PSED.

3.1 Error-based Quality Metric

After compression, a set of consecutive line segments is used to approximately represent each raw trajectory. For a good compression algorithm, the deviation between these line segments and the raw trajectory should be as small as possible. How to calculate the deviation calls for a more reasonable error-based quality metric. Usually, the deviation is calculated based on the distance between every raw point and its corresponding line segment. PED, an error-based quality metric, is adopted by most existing line simplification methods, e.g. [10, 15–18, 21]. PED measures the deviation between the raw trajectory and its compressed trajectory by calculating the shortest euclidean distance from each discarded point to the straight line on which the corresponding line segment of this discarded point lies. The formal definition is shown as follows:

Definition 3.1. (Perpendicular Euclidean Distance (PED)): Given a trajectory segment $T[s : e] (s < e)$, the line segment $p_s p_e$ is the compressed form of $T[s : e]$. For any discarded point $p_m (s < m < e)$ in $T[s : e]$, the PED of p_m can be calculated as follows:

$$\begin{aligned} PED(p_m) &= \frac{\|\overrightarrow{p_s p_m} \times \overrightarrow{p_s p_e}\|}{\|\overrightarrow{p_s p_e}\|} \\ &= \frac{|(x_m - x_s)(y_e - y_s) - (x_e - x_s)(y_m - y_s)|}{\sqrt{(x_e - x_s)^2 + (y_e - y_s)^2}}, \end{aligned}$$

where \times is the symbol of cross product in vector operations and $\|\cdot\|$ is to calculate the length of a vector.

Though PED can be applied in the many cases, there are still some cases where it's particularly unreasonable, for example, the direction of the tracked object changes greatly, e.g. a pedestrian is strolling in a shopping mall or a car is running on the spiral highway. Figure 1 illustrates an example that the tracked object makes an u-turn and the line segment $p_1 p_6$ approximately represents raw trajectory points p_1, p_2, \dots, p_6 . Based on Definition 3.1, we can calculate the difference between every discarded raw trajectory point and its corresponding line segment. $PED(p_2) = PED(p_5) = 0$, $PED(p_3) = |p_3 p'_3|$ and $PED(p_4) = |p_4 p'_4|$. Raw trajectory points have been compressed into multiple consecutive line segments, but not straight lines. It sounds unreasonable that $PED(p_3) = |p_3 p'_3|$ just because the vertical dimension between p_3 and the extension line of the line segment $p_1 p_6$ is $|p_3 p'_3|$. It's particularly obvious that p_2 is far from the line segment $p_1 p_6$, but $PED(p_2) = 0$.

Every raw trajectory has been compressed into a set of consecutive line segments, and this set of consecutive line segments, but not straight lines, approximately describes the movement of

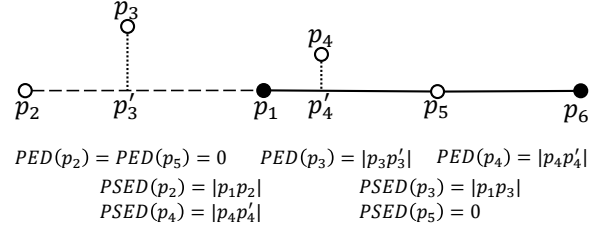


Figure 1: The trajectory segment $T[1 : 6]$ has been compressed into the line segment $p_1 p_6$. This example is to show how to calculate PED and PSED.

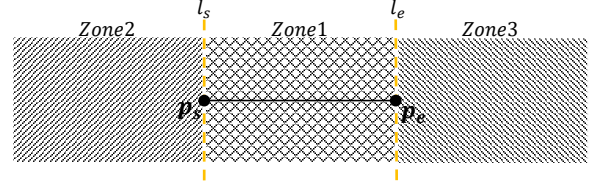


Figure 2: Partition the whole planar space into 3 zones.

the tracked object. PED is defective in many cases since the calculations of PED are still based on the shortest euclidean distance from each discarded point to the straight line on which the corresponding line segment of this discarded point lies. In this paper, we propose a new error-based quality metric, point-to-segment euclidean distance (PSED for short). PSED is an error criterion based on the shortest euclidean distance from a point to its corresponding line segment. Given a discarded trajectory point p_m and its corresponding line segment $p_s p_e$ after the compression, we first get two vertical lines l_s and l_e perpendicular to $p_s p_e$ as shown in Figure 2, where the intersections are p_s and p_e respectively. l_s and l_e partition the whole planar space into three parts, i.e. *Zone1*, *Zone2* and *Zone3*. p_m may be in any one of these three zones, and $PSED(p_m)$ can be calculated in different situations: (1) If p_m is in *Zone1*, $PSED(p_m)$ is the vertical distance from p_m to $p_s p_e$, the same as $PED(p_m)$. (2) If p_m is in *Zone2*, $|p_m p_s|$ is the minimum distance from p_m to $p_s p_e$ and $PSED(p_m) = |p_m p_s|$. (3) Similar to the case that p_m is in *Zone2*, if p_m is in *Zone3*, $PSED(p_m) = |p_m p_e|$. The formal definition of PSED is shown as follows:

Definition 3.2. (Point-to-segment Euclidean Distance (PSED)): Given a trajectory segment $T[s : e] (s < e)$, the line segment $p_s p_e$ is the compressed form of $T[s : e]$. For any discarded point $p_m (s < m < e)$ in $T[s : e]$, the PSED of p_m is calculated according to the following cases:

$$PSED(p_m) = \begin{cases} \frac{\|\overrightarrow{p_s p_m} \times \overrightarrow{p_s p_e}\|}{\|\overrightarrow{p_s p_e}\|} & \overrightarrow{p_s p_m} \cdot \overrightarrow{p_s p_e} \geq 0 \text{ and } \overrightarrow{p_m p_e} \cdot \overrightarrow{p_s p_e} \geq 0 \\ |p_s p_m| & \overrightarrow{p_s p_m} \cdot \overrightarrow{p_s p_e} < 0 \\ |p_m p_e| & \overrightarrow{p_m p_e} \cdot \overrightarrow{p_s p_e} < 0 \end{cases},$$

where \times and \cdot are respectively the symbol of cross product and dot product in vector operations. When both $\overrightarrow{p_s p_m} \cdot \overrightarrow{p_s p_e} \geq 0$ and $\overrightarrow{p_m p_e} \cdot \overrightarrow{p_s p_e} \geq 0$ are satisfied, p_m must be in *Zone1*, and $PSED(p_m)$ is the same as $PED(p_m)$.

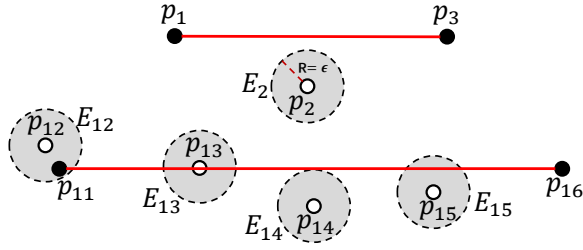


Figure 3: $T_1 = \{p_1, p_2, p_3\}$ and $T_2 = \{p_{12}, p_{13}, \dots, p_{16}\}$ are two raw trajectories and have been compressed into $\{p_1 p_3\}$ and $\{p_{11} p_{16}\}$ respectively.

In Figure 1, since p_2 and p_3 are both in Zone_2 of $p_1 p_6$, $\text{PSED}(p_2) = |p_1 p_2|$ and $\text{PSED}(p_3) = |p_1 p_3|$. Since p_4 and p_5 are both in Zone_1 , $\text{PSED}(p_4) = \text{PED}(p_4) = |p_4 p'_4|$ and $\text{PSED}(p_5) = \text{PED}(p_5) = 0$.

With the definition of PSED, the ϵ -error-bounded trajectory is defined as follows:

Definition 3.3. (ϵ -Error-bounded Trajectory): Given the error tolerance ϵ , a raw trajectory $T = \{p_1, p_2, \dots, p_N\}$ and its compressed trajectory $T' = \{p_{i_1}, p_{i_2}, \dots, p_{i_n}\}$ ($p_{i_1} = p_1, p_{i_n} = p_N$). If \forall discarded point $p_m \in T$, $\text{PSED}(p_m) \leq \epsilon$, and then we say T' is ϵ -error-bounded.

3.2 Algorithm ROCE

In this part, we present a new trajectory compression algorithm ROCE. Given a raw trajectory $T = \{p_1, p_2, \dots, p_N\}$ and the error tolerance ϵ , ROCE is to compress such a raw trajectory into an ϵ -error-bounded compressed trajectory T' , which is made up of multiple consecutive line segments.

First we present a new concept ϵ -Region as below:

Definition 3.4. (ϵ -Region): Given the error tolerance ϵ and a raw trajectory point p_i , we can get a circle whose center is p_i and radius is ϵ . This circle is the corresponding ϵ -Region of p_i .

E_i is used to denote the corresponding ϵ -Region of p_i . Given a raw trajectory point p_i and its corresponding ϵ -Region E_i and line segment $p_s p_e$ ($s < i < e$) after the compression, if $p_s p_e$ intersects E_i , then p_i can be approximately represented by $p_s p_e$ according to Definition 3.3. In Figure 3, T_1 has been compressed into $T'_1 = \{p_1 p_3\}$. For the discarded point p_2 , we can get its corresponding ϵ -Region E_2 . It's obvious that the line segment $p_1 p_3$ doesn't intersect E_2 and $\text{PSED}(p_2) > \epsilon$. Thus T'_1 isn't ϵ -error-bounded. T_2 has been compressed into $T'_2 = \{p_{11} p_{16}\}$. For all discarded points, the line segment $p_{11} p_{16}$ intersects all their corresponding ϵ -Regions and the PSEDs of these discarded points are all no more than ϵ . Only such a compressed trajectory meets the requirement of Definition 3.3. From this example, we can sum up a property as below:

LEMMA 3.5. Given a trajectory segment $T[i : i + m]$ and the error tolerance ϵ , $T[i : i + m]$ has been compressed into a line segment $p_i p_{i+m}$. $p_i p_{i+m}$ is ϵ -error-bounded iff $p_i p_{i+m}$ intersects all ϵ -Regions of all discarded points, i.e. $E_{i+1}, E_{i+2}, \dots, E_{i+m-1}$.

If we want to increase the compression rate, all we need is to make every line segment intersects as many ϵ -Regions of continuous trajectory points as possible. Given a raw trajectory $T =$

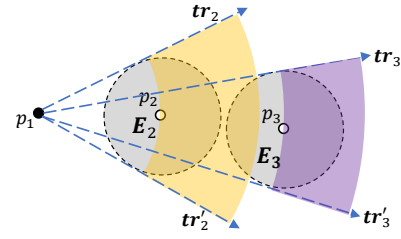


Figure 4: An example about how to update the candidate region.

$\{p_1, p_2, \dots, p_N\}$ and the error tolerance ϵ , the optimal compression is to compress T into an ϵ -error-bounded trajectory T' which consists of the smallest number of consecutive line segments. T can be split into 2^{N-1} different sets of consecutive trajectory segments, each of which is compressed into a line segment. Hence, the cost of finding the optimal compression is particularly high. In order to reduce the time cost greatly with just constant space, ROCE uses a greedy strategy and some effective tricks to handle the trajectory compression in an online processing manner. The greedy strategy of ROCE is to compress as many continuous trajectory points as possible from the last trajectory point in the compressed part (from the first point in the uncompressed part in the first time) by using only one line segment. In order to avoid that every raw trajectory point is scanned multiple times in the compression, ROCE adopts the candidate region where endpoints of the ϵ -Error-bounded line segments starting from p_i are, which is formally defined as follows:

Definition 3.6. (Candidate Region): Given the error tolerance ϵ , a raw trajectory point p_i where the ϵ -Error-bounded line segment starts after the compression, and another raw trajectory point p_j ($i < j$ and $|p_i p_j| > \epsilon$), we can get the corresponding ϵ -Region E_j of p_j . Since p_i is outside E_j , we can get two tangent rays of E_j starting from p_i and named tr_j and tr'_j respectively. The whole sector which consists of two rays tr_j and tr'_j , except the region whose distance from p_i is no more than $|p_i p_j|$, is the candidate region where endpoints of the ϵ -Error-bounded line segments starting from p_i are.

As shown in Figure 4, since p_1 is outside the corresponding ϵ -Region E_2 of p_2 , we can get two tangent rays tr_2 and tr'_2 of E_2 starting from p_1 . To satisfy the error constraint, we stipulate that each ϵ -error-bounded line segment to be compressed from its corresponding trajectory segment shouldn't get shorter and shorter as the number of trajectory points in this trajectory segment increases. Then the candidate region is the region in orange. Because of the candidate region, each raw trajectory point needs to be scanned only once, and ROCE only needs just constant and small space to store such a candidate region, but not trajectory points or their corresponding ϵ -Regions, no matter how many trajectory points to be compressed into a line segment. When we get the next point p_3 and $|p_1 p_3| \geq |p_1 p_2|$, we can get the new candidate region which is the region in purple according to Definition 3.6. The overlapped region of the original candidate region and the new candidate region is the final candidate region updated by p_3 , and it's just coincidental that the final candidate region is also the region in purple.

ROCE is formally described in Algorithm 1. Each time ROCE starts to compress a new trajectory segment into a line segment, it must first use $Initialize(CandidateRegion, StartPoint)$ to initialize $CandidateRegion$ to a circle whose center is $StartPoint$ and radius is infinite (Line 3,14 and 23). And then, ROCE compresses as many continuous trajectory points as possible from the last trajectory point in the compressed part (from the first point in the uncompressed part in the first time) by using only one line segment (Lines 4-26). Lines 5-7 are used to accelerate in a particular case that the tracked object remains in the same place. If $StartPoint$ is in all ϵ -Regions of the previous trajectory points, any line segment starting from $StartPoint$ must intersect all these ϵ -Regions and we don't need to care about these previous points (Lines 8-10). To satisfy the error constraint, each ϵ -error-bounded line segment to be compressed from its corresponding trajectory segment shouldn't get shorter as the number of trajectory points in this trajectory segment increases (Lines 11-15). If the condition in Line 17 is satisfied, Roce needs to update $CandidateRegion$. Roce needs to repeat these processes until the last point of T has been processed. Lines 27-29 are used to append the last line segment to the final result set.

Algorithm 1 The ROCE Algorithm

Require: Raw trajectory $T = \{p_1, p_2, \dots, p_N\}$, error tolerance ϵ
Ensure: ϵ -Error-bounded trajectory $T' = \{p_{i_1}, p_{i_2}, \dots, p_{i_n}\} (p_{i_1} = p_1, p_{i_n} = p_N)$ of T

- 1: $LastPoint = StartPoint = T[1]$
- 2: $T' = [StartPoint]$
- 3: $Initialize(CandidateRegion, StartPoint)$
- 4: **for** $Point$ in $T[2, T.length()]$ **do**
- 5: **if** $T[i] == LastPoint$ **then**
- 6: continue
- 7: **end if**
- 8: **if** $StartPoint$ in $EpsilonRegion(Point, \epsilon)$ **then**
- 9: **if** $StartPoint$ in $EpsilonRegion(LastPoint, \epsilon)$ **then**
- 10: continue
- 11: **else**
- 12: $T'.Append(LastPoint)$
- 13: $StartPoint = LastPoint$
- 14: $Initialize(CandidateRegion, StartPoint)$
- 15: **end if**
- 16: **else**
- 17: **if** $Point$ in $CandidateRegion$ **then**
- 18: $LastPoint = Point$
- 19: $UpdateCandidateRegion(CandidateRegion, Point, \epsilon)$
- 20: **else**
- 21: $T'.Append(LastPoint)$
- 22: $StartPoint = LastPoint$
- 23: $Initialize(CandidateRegion, StartPoint)$
- 24: **end if**
- 25: **end if**
- 26: **end for**
- 27: **if** $T'[T'.length()] \neq T[T.length()]$ **then**
- 28: $T'.Append(T[T.length()])$
- 29: **end if**
- 30: **return** T'

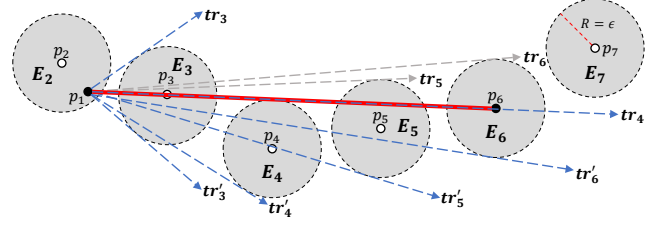


Figure 5: The processing procedure of ROCE.

Figure 5 gives an example to show the processing procedure of the compression algorithm ROCE. ROCE starts from the first trajectory point p_1 in the uncompressed part and initializes the candidate region. Then we get the next point p_2 , and the line segment p_1p_2 must meet the error constraint requirement because there is no discarded point. Since the ϵ -Region E_2 contains p_1 , any line segment with p_1 as its one endpoint must intersect E_2 . Thus we don't need to think about the restrictions of E_2 . When p_3 comes and its corresponding ϵ -Region E_3 doesn't contain p_1 , then we update the candidate region based on E_3 . ROCE repeats to update the candidate region when p_4, p_5 and p_6 arrive. Since p_7 is outside the candidate region, which means p_1p_7 isn't ϵ -Error-bounded, we should compress $T[1 : 6]$ into the line segment p_1p_6 , and restart another similar processing procedure from p_6 until the last point of this trajectory has been compressed.

It's obvious that ROCE is a one-pass error bounded trajectory compression algorithm, which scans each trajectory point in a trajectory once and only once. So the time complexity of ROCE is $O(N)$. Since ROCE only needs to store and update the candidate region $CandidateRegion$ and two points $StartPoint$ and $LastPoint$ in the local buffer, the space complexity of ROCE is $O(1)$.

4 RANGE QUERY

4.1 Range Query Algorithm based on Line Segments

Definition 4.1. (Range Query on Compressed Trajectories): Given a compressed trajectory dataset \mathbb{T} and a rectangular query region R , whose edges are either horizontal or vertical, a range query $Q_r(R)$ returns all compressed trajectories, at least one of whose line segment overlaps R .

Definition 4.1 is different from the old definition defined by previous work which thinks a trajectory overlaps the query region R iff at least one point of this trajectory is in R . The old definition is especially not applicable to the situation where the query trajectories are compressed trajectories consisting of multiple continuous line segments with different lengths. Each trajectory segment may represent hundreds of raw trajectory points and be dozens of kilometers. Let's see an example. A trajectory T goes straight through the query region R with all trajectory points in R , except the starting point and the ending point. The compressed trajectory T' of T , which consists of only one line segment, still doesn't overlap R according to the old definition, because neither endpoint of this line segment is in R . But based on Definition 4.1, T' can be found in the result set.

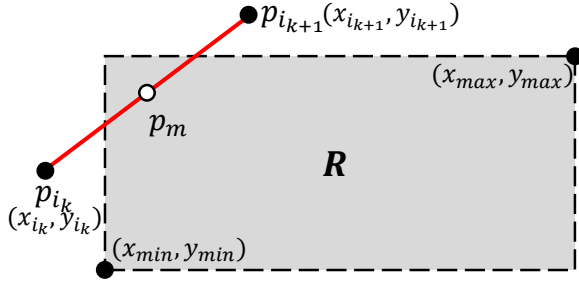


Figure 6: An example that neither endpoint of the line segment $p_{i_k}p_{i_{k+1}}$ is in region R , but $p_{i_k}p_{i_{k+1}}$ and R overlap.

Substantial experiments have been done in Section 6.3.1 and the result is that range queries based on segments are up to 10.3% more accurate than the ones based on points. This result and the example described in the last paragraph both illustrate that the range queries based on trajectory points are no longer suitable for compressed trajectories, and the range queries based on line segments are needed here. In addition, it's also more reasonable to use consecutive line segments to approximately describe the real movement path of the tracked object.

Given a range query rectangular region R and a line segment $p_{i_k}p_{i_{k+1}}$, the coordinates of R , p_{i_k} and $p_{i_{k+1}}$ are shown in Figure 6. It's easy for us to determine whether $p_{i_k}p_{i_{k+1}}$ overlaps R when at least one of p_{i_k} and $p_{i_{k+1}}$ is in R .

(1) If at least one of p_{i_k} and $p_{i_{k+1}}$ is in R , i.e. at least one of these two inequality groups

$$\begin{cases} x_{min} \leq x_{i_k} \leq x_{max} \\ y_{min} \leq y_{i_k} \leq y_{max} \end{cases} \quad \begin{cases} x_{min} \leq x_{i_{k+1}} \leq x_{max} \\ y_{min} \leq y_{i_{k+1}} \leq y_{max} \end{cases}$$

can be satisfied, $p_{i_k}p_{i_{k+1}}$ must overlap R .

However, that neither of these two endpoints is in R doesn't mean that $p_{i_k}p_{i_{k+1}}$ doesn't overlap R as shown in Figure 6 and the example mentioned just now. Given the coordinates of two endpoints $p_{i_k}(x_{i_k}, y_{i_k})$ and $p_{i_{k+1}}(x_{i_{k+1}}, y_{i_{k+1}})$, first, we need to make sure that $x_{i_k} \leq x_{i_{k+1}}$, otherwise exchange the coordinates of p_{i_k} and $p_{i_{k+1}}$ to ensure that $x_{i_k} \leq x_{i_{k+1}}$. This can make calculations more simple. $p_m(x_{i_k} + t(x_{i_{k+1}} - x_{i_k}), y_{i_k} + t(y_{i_{k+1}} - y_{i_k}))$ can be used to represent any point on the line segment $p_{i_k}p_{i_{k+1}}$, where t is a variable and $0 \leq t \leq 1$. So $p_{i_k}p_{i_{k+1}}$ overlaps R iff the inequality group

$$\begin{cases} x_{min} \leq x_{i_k} + t(x_{i_{k+1}} - x_{i_k}) \leq x_{max} \\ y_{min} \leq y_{i_k} + t(y_{i_{k+1}} - y_{i_k}) \leq y_{max} \\ 0 \leq t \leq 1 \end{cases} \quad (1)$$

can be satisfied. Equation 1 can be further simplified to

$$\begin{cases} x_{min} - x_{i_k} \leq t(x_{i_{k+1}} - x_{i_k}) \leq x_{max} - x_{i_k} \\ y_{min} - y_{i_k} \leq t(y_{i_{k+1}} - y_{i_k}) \leq y_{max} - y_{i_k} \\ 0 \leq t \leq 1 \end{cases} \quad (2)$$

Now, let's discuss the situations separately.

(2) If Condition (1) can't be satisfied, $x_{i_k} < x_{i_{k+1}}$ and $y_{i_k} < y_{i_{k+1}}$, we define two variables $tv_1 = \max \left\{ \frac{x_{min} - x_{i_k}}{x_{i_{k+1}} - x_{i_k}}, \frac{y_{min} - y_{i_k}}{y_{i_{k+1}} - y_{i_k}} \right\}$, $tv_2 = \min \left\{ \frac{x_{max} - x_{i_k}}{x_{i_{k+1}} - x_{i_k}}, \frac{y_{max} - y_{i_k}}{y_{i_{k+1}} - y_{i_k}} \right\}$ at first. $p_{i_k}p_{i_{k+1}}$ overlaps R iff the inequality group

$$\begin{cases} tv_1 \leq tv_2 \\ tv_1 \leq 1 \\ tv_2 \geq 0 \end{cases}$$

can be satisfied.

(3) If Condition (2) can't be satisfied, $x_{i_k} < x_{i_{k+1}}$ and $y_{i_k} > y_{i_{k+1}}$, we define two variables $tv_3 = \max \left\{ \frac{x_{min} - x_{i_k}}{x_{i_{k+1}} - x_{i_k}}, \frac{y_{max} - y_{i_k}}{y_{i_{k+1}} - y_{i_k}} \right\}$, $tv_4 = \min \left\{ \frac{x_{max} - x_{i_k}}{x_{i_{k+1}} - x_{i_k}}, \frac{y_{min} - y_{i_k}}{y_{i_{k+1}} - y_{i_k}} \right\}$ at first. $p_{i_k}p_{i_{k+1}}$ overlaps R iff the inequality group

$$\begin{cases} tv_3 \leq tv_4 \\ tv_3 \leq 1 \\ tv_4 \geq 0 \end{cases}$$

can be satisfied.

(4) If Condition (3) can't be satisfied, $x_{i_k} < x_{i_{k+1}}$ and $y_{i_k} = y_{i_{k+1}}$, $p_{i_k}p_{i_{k+1}}$ overlaps R iff the inequality group

$$\begin{cases} y_{min} \leq y_{i_k} \leq y_{max} \\ x_{i_k} \leq x_{max} \\ x_{min} \leq x_{i_{k+1}} \end{cases}$$

can be satisfied.

(5) If Condition (4) can't be satisfied and $x_{i_k} = x_{i_{k+1}}$, then $p_{i_k}p_{i_{k+1}}$ overlaps R iff one of two inequality groups

$$\begin{cases} x_{min} \leq x_{i_k} \leq x_{max} \\ y_{i_k} \leq y_{i_{k+1}} \\ y_{i_k} \leq 1 \\ y_{i_{k+1}} \geq 0 \end{cases} \quad \begin{cases} x_{min} \leq x_{i_k} \leq x_{max} \\ y_{i_{k+1}} \leq y_{i_k} \\ y_{i_k} \geq 0 \\ y_{i_{k+1}} \leq 1 \end{cases}$$

can be satisfied.

These 5 conditions can cover all cases which might happen. However, there are quite a lot of line segments whose two endpoints are neither in R . Though most of them don't meet the situation similar to the one shown in Figure 6, we still need some slightly complicated calculations to exclude them. In view of this kind of situations, we come up with an acceleration strategy. It's quite easy to be understood that if two endpoints of a line segment are both above the straight line $(x_{min}, y_{max})(x_{max}, y_{max})$, this line segment must not overlap R . There are also similar properties below the straight line $(x_{min}, y_{min})(x_{max}, y_{min})$, to the left of the straight line $(x_{min}, y_{min})(x_{min}, y_{max})$ and to the right of the straight line $(x_{max}, y_{min})(x_{max}, y_{max})$. Since it's much easier to be judged, we can use these properties first to speed up the validation of the relationship between each line segment and the query region R . The formal description is shown as below:

(0) If at least one of four inequality groups

$$\begin{cases} y_{max} < y_{i_k} \\ y_{max} < y_{i_{k+1}} \\ x_{i_k} < x_{min} \\ x_{i_{k+1}} < x_{min} \end{cases} \quad \begin{cases} y_{i_k} < y_{min} \\ y_{i_{k+1}} < y_{min} \\ x_{max} < x_{i_k} \\ x_{max} < x_{i_{k+1}} \end{cases}$$

can be satisfied, $p_{i_k}p_{i_{k+1}}$ must not overlap R .

Condition (0) is used to show the highest priority to be calculated. After experimental verification in Section 6.3.3, this acceleration strategy can accelerate up to 14.6%.

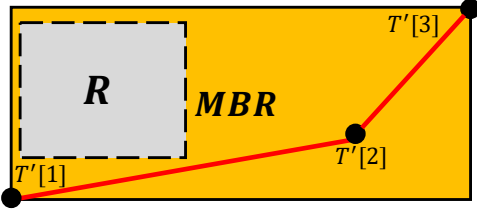


Figure 7: The gray rectangle is on behalf of the query region R and the orange rectangle represents the $MBR(T')$ of the compressed trajectory T' .

In order to answer $Q_r(R)$ on compressed trajectories, by using the method discussed above, we have to verify the relationship between each line segment of a compressed trajectory T' and the query region R . But can we directly determine whether T' overlaps R in some cases? Under our efforts, the answer is yes. First, we will give the definition of the minimum boundary rectangle (MBR for short), which will be used later. $MBR(T')$ is the smallest rectangle containing the entire compressed trajectory T' , whose edges are either horizontal or vertical. The formalized definition of MBR is shown as follows:

Definition 4.2. (Minimum Boundary Rectangle (MBR): Given a compressed trajectory T' , its corresponding MBR, $MBR(T')$, is a rectangle, the coordinate of whose lower left corner is $(\min\{T'.x\}, \min\{T'.y\})$ ($\min\{T'.x\}$ ($\min\{T'.y\}$) is the minimum x (y) coordinate value in all endpoints of T' 's line segments. Similarly, for $MBR(T')$, the coordinate of its upper right corner is $(\max\{T'.x\}, \max\{T'.y\})$, where $\max\{T'.x\}$ ($\max\{T'.y\}$) is the maximum x (y) coordinate value in all endpoints of T' 's line segments.

We can easily get a theorem as below:

THEOREM 4.3. *If $MBR(T')$ doesn't overlap the query region R , it's sure that T' and R don't overlap, but the reverse is not always true.*

It's quite obvious that T' and R must not overlap if $MBR(T')$ doesn't overlap the query region R . But if $MBR(T')$ and R overlap, it's not sure whether T' overlaps R , such as the situation shown in Figure 7.

After serious thinking, when $MBR(T')$ and R overlap, there are still 3 cases where T' must overlap R without the need for verifying the relationship between each line segment of T' and the query region R . These 3 cases are shown in Figure 8. In the first subimage, $MBR(T')$ is contained by R and there is no doubt that T' overlaps R . In the second subimage, $MBR(T')$ has only one whole edge enclosed by R . From Definition 4.2, we can get that there is at least one endpoint of T' is on each edge of $MBR(T')$. So at least one endpoint of T' is in R and T' must overlap R . In the last subimage, two parallel edges of $MBR(T')$ overlap R , but neither of the other two parallel edges is in R . From the analysis of the second subimage, we should know that there are both at least one endpoint of T' on $MBR(T')$'s parallel edges which don't overlap R . Since T' consists of multiple continuous line segments, any two endpoints of T' are connected by at least one continuous line segment, so do these two points in the last sentence. In other words, there must be at least one line segment of T' overlapping R . So T' must overlap R in the last subimage.

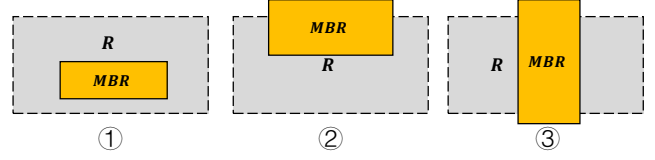


Figure 8: Each gray rectangle is on behalf of the query region R and each orange rectangle represents the $MBR(T')$ of a compressed trajectory T' .

After careful summary and simplification about the above 3 cases, the formal description of this property is shown as follows:

THEOREM 4.4. *Given the query region R and a compressed trajectory T' , the coordinates of $MBR(T')$ can be calculated. x_{max} , x_{min} , y_{max} and y_{min} are used to represent the maximum and minimum horizontal and vertical coordinates of R respectively. Similarly, x'_{max} , x'_{min} , y'_{max} and y'_{min} are used to represent the maximum and minimum horizontal and vertical coordinates of $MBR(T')$ respectively. If at least one of two inequality groups*

$$\begin{cases} x_{min} \leq x'_{min} \\ x'_{max} \leq x_{max} \\ y'_{min} \leq y_{max} \\ y_{min} \leq y'_{max} \end{cases} \quad \begin{cases} y_{min} \leq y'_{min} \\ y'_{max} \leq y_{max} \\ x'_{min} \leq x_{max} \\ x_{min} \leq x'_{max} \end{cases}$$

can be satisfied, T' must overlap R .

Theorem 4.3 and Theorem 4.4 should be used before Condition (0), (1),..., (5), and they can accelerate range queries on compressed trajectories obviously. By just using Theorem 4.4, the speedup is up to 23.1% according to the results of the experiment in Section 6.3.3.

4.2 Spatial Index BPA

Section 4.1 has introduced a whole set of solutions to answer range queries on compressed trajectories. However, we still need to determine the relationship between the query region R and each compressed trajectory, or even R and each line segment one by one. Can we directly determine the relationship between the query region R and a batch of compressed trajectories in some situations to speed up range queries?

In order to solve this problem, we put forward a balanced spatial partition quadtree index (BPA for short). The space partition varies with the compressed trajectories themselves. First, we use an array large enough to hold the entire compressed trajectory dataset \mathbb{T} . The order of storage is based on the ids of all compressed trajectories. By using only the starting and ending offset addresses, we can represent any compressed trajectory or sub-trajectory in BPA.

Figure 9 helps us to understand BPA more intuitively. In the top half of this picture, there is a three-tier index tree of BPA. But in real applications, the number of BPA's levels is usually greater than 3. At the first level of BPA, there is only one node, the root node, which represents the whole rectangular region as indicated by the blue arrow. The root node contains the entire compressed trajectory dataset \mathbb{T} . Each node of BPA has 4 child nodes if this node has at least ξ line segments, or this node is a leaf node. ξ is a threshold value given by the user. How to ensure that BPA is well balanced? Here, we adopt a data adaptive strategy. Before a father node is

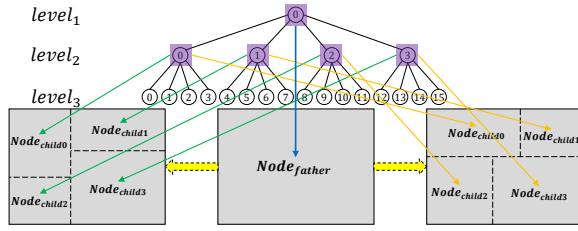


Figure 9: The structure of BPA.

split into 4 child nodes, we first get all endpoints of line segments in this father node, and then calculate the median value of all x -axis (y -axis) values. We use the result of this calculation to draw a vertical (horizontal) line and this line splits the corresponding rectangular region of the father node into two parts. Then, the median values of the y -axis (x -axis) values in these two parts are respectively used to further split these two parts into four parts as shown in this figure. After the rectangular region of the father node is divided, the line segments of the father node should also be divided among its 4 child nodes. How to divide these line segments will be introduced later. There are two ways of cutting a father node in total, and the one with the smaller total number of line segments after the cuts is chosen. Proved by the experiment in Section 6.3.4, the results show that this partitioning strategy dose work and BPA is well balanced.

Let's introduce how to divide line segments of a father node among its 4 child nodes. The basic strategy is to verify which one or more rectangular regions in these 4 child nodes each line segment intersects, and then assign this line segment to the corresponding child nodes. Figure 10 gives us an example on how to divide a compressed trajectory or sub-trajectory T'_i among 4 child nodes of a father node. T'_i consists of 4 line segments, i.e. $T'_i[k+1]T'_i[k+2]$, $T'_i[k+2]T'_i[k+3]$, $T'_i[k+3]T'_i[k+4]$ and $T'_i[k+4]T'_i[k+5]$. Let's assume that the offset of $T'_i[k+1]$ in the array just introduced is $m+1$ and the key-value pair $(m+5) \rightarrow (m+1, i)$ is used to represent T'_i . This representation can save lots of space and help us to merge consecutive line segments conveniently. At first, we initialize each of these four child nodes with an empty dictionary $\{ \}$. When the line segment $T'_i[k+1]T'_i[k+2]$, i.e. $(m+2) \rightarrow (m+1, i)$, comes, $T'_i[k+1]T'_i[k+2]$ only overlaps $Node_{child3}$, so the dictionary of $Node_{child3}$ becomes $\{(m+2) \rightarrow (m+1, i)\}$. When the line segment $T'_i[k+2]T'_i[k+3]$, i.e. $(m+3) \rightarrow (m+2, i)$, comes, $T'_i[k+2]T'_i[k+3]$ overlaps $Node_{child0}$, $Node_{child1}$ and $Node_{child3}$, so the dictionarys of $Node_{child0}$ and $Node_{child1}$ both become $\{(m+3) \rightarrow (m+2, i)\}$. As for $Node_{child3}$, we should check whether there is an element whose key is equal to $m+2$ and corresponding trajectory id is equal to i in the dictionary of $Node_{child3}$. The result is yes, and then the dictionary of $Node_{child3}$ is updated to $\{(m+3) \rightarrow (m+1, i)\}$. Similarly when we are dealing with the line segment $T'_i[k+3]T'_i[k+4]$, i.e. $(m+4) \rightarrow (m+3, i)$, the dictionarys of $Node_{child0}$ and $Node_{child2}$ are updated to $\{(m+4) \rightarrow (m+2, i)\}$ and $\{(m+4) \rightarrow (m+3, i)\}$ respectively. When we deal with the last line segment $T'_i[k+4]T'_i[k+5]$, i.e. $(m+5) \rightarrow (m+4, i)$, it overlaps $Node_{child2}$ and $Node_{child3}$. The dictionary of $Node_{child2}$ is finally updated to $\{(m+5) \rightarrow (m+3, i)\}$. However, the dictionary of $Node_{child3}$ finally becomes $\{(m+3) \rightarrow (m+1, i), (m+5)$

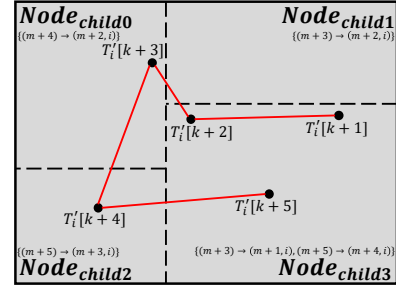


Figure 10: An example that a compressed trajectory or sub-trajectory in a father node is split among its 4 child nodes.

$\rightarrow (m+4, i)$ }, because there is no key equal to $m+4$ in the dictionary of $Node_{child3}$.

In the last example, it's worth to be noticed that though there is a line segment $T'_i[k+2]T'_i[k+3]$ in $Node_{child1}$, there are no endpoints in this node. If this kind of nodes are needed to be further split into 4 child nodes, we should use the horizontal and vertical midlines of this region, instead of the lines described above, to divide this kind of regions.

In order to reduce BPA's space overhead, all the line segments in each father node will be removed after this father node has been split among its 4 child nodes. When BPA has been built completely, only leaf nodes store line segments.

Let's make a summary about how to answer a range $Q_r(R)$ on compressed trajectories with BPA. First, traverse BPA from top to bottom with the query region R to find all leaf nodes overlapping R , and put the *ids* of all compressed trajectories or sub-trajectories contained by these leaf nodes directly into the candidate set. If a non-leaf node doesn't overlap R , all descendants of this node are no longer needed to be traversed. Find the leaf nodes whose corresponding regions are completely contained by R , and then put the corresponding *ids* into the result set. Second, use the *MBR* of each compressed trajectory or sub-trajectory in the rest candidate set to determine the relationship between the query region R and this compressed trajectory or sub-trajectory one by one. Third, if we still can't judge whether a compressed trajectory or sub-trajectory overlaps R , we have to check whether there is at least one line segment of this compressed trajectory or sub-trajectory overlaps the query region R . After these three steps, we can get the final result of $Q_r(R)$.

5 SIMILARITY QUERY

There is no doubt that how to quantify the similarity between two compressed trajectories is the most fundamental operation in the process of answering similarity queries on compressed trajectories. Therefore, in Section 5.1, a new error-based quality metric AL will be introduced first, and then we will introduce how to answer top- k similarity queries on compressed trajectories in Section 5.2.

5.1 Error-based Quality Metric AL

Most widely used trajectory distance metrics only focus on the distance between matched point pairs of two trajectories. This

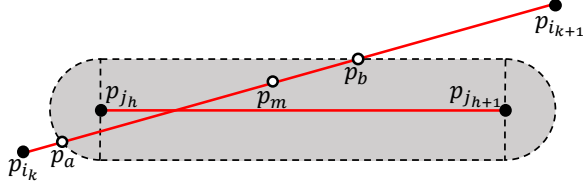


Figure 11: An example that the matched line segment $p_{j_h}p_{j_{h+1}}$ is used to cut $p_{i_k}p_{i_{k+1}}$. Both the diameter of the gray semicircles and the width of the gray rectangle are 2σ .

strategy may be reasonable for the situations where the distance between consecutive point pairs of a single trajectory doesn't change much. But these distance metrics are not suitable for compressed trajectories, because each compressed trajectory consists of multiple continuous line segments and the length of each line segment varies greatly. Suppose we have two pairs of matched line segments, the lengths of the first pair are both $10km$, the lengths of the second pair are both $0.1km$, and the distances between these 4 matched endpoint pairs are exactly the same. Should we quantify the distances between these two pairs of line segments to be the same? Obviously, it's better not to do so, and the lengths of matched line segments should also be considered when we quantify the distance between each pair of compressed trajectories. Inspired by this, we propose a new distance metric Area sandwiched by the Line segments of trajectories (AL for short). AL uses the area sandwiched by pairs of line segments to describe how two compressed trajectories are similar.

Suppose we have two compressed trajectories R' and S' , and S' is a sub-trajectory of R' . It seems to be more reasonable that S' is matched with its corresponding sub-trajectory of R' and we punish those unmatched line segments, rather than like DTW, another trajectory similarity measure, in which each endpoint of R' and S' must be matched with an endpoint of the other trajectory.

Only when the minimum distance between two line segments is less than a given distance threshold value σ , can these two line segments be considered to have some similarities. Otherwise, they can't be matched with each other. In order to avoid the appearance of such a situation that the area sandwiched by a pair of matched line segments is greater than the penalty costs of these two line segments, we cut each matched line segment into at most two parts. The first part must be a subline segment and the minimum distance from each point on this subline segment to its matched line segment is no more than σ . The second part is the remaining one or two subline segments of this line segment, if the first part is not this line segment itself. As shown in Figure 11, if $p_{i_k}p_{i_{k+1}}$ is matched with $p_{j_h}p_{j_{h+1}}$, the first part of $p_{i_k}p_{i_{k+1}}$ is $p_a p_b$, and the second part is the line segments $p_{i_k} p_a$ and $p_b p_{i_{k+1}}$.

We only need to calculate the area sandwiched by two first parts and the penalty costs of two second parts in each pair of matched line segments. After that, the sum of these two results is used to describe the distance between these two matched line segments.

When we calculate the area sandwiched by two first parts of matched line segments, there are mainly 5 cases as shown in Figure 12. $p_a p_b$ and $p_c p_d$ are used to be on behalf of two first parts of matched line segments here. S_{abc} represents the area of the triangle

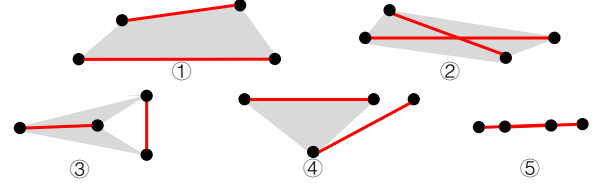


Figure 12: An example to show how to calculate the area sandwiched by two first parts of matched line segments.

whose three vertices are p_a, p_b and p_c , and S is used to represent the area sandwiched by $p_a p_b$ and $p_c p_d$. The result S can be calculated in different situations:

- (1) If $p_a p_b p_c p_d p_a$ is a convex hull made up of four line segments $p_a p_b, p_b p_c, p_c p_d$ and $p_d p_a$, then $S = S_{abd} + S_{bcd}$.
- (2) If $p_a p_b p_d p_c p_a$ is a convex hull made up of four line segments $p_a p_b, p_b p_d, p_d p_c$ and $p_c p_a$, then $S = S_{abd} + S_{acd}$.
- (3) If neither of Condition (1) or Condition (2) can be satisfied, and two points p_c and p_d are on different sides of the straight line $p_a p_b$, then $S = S_{abc} + S_{abd}$.
- (4) If Condition (3) is not satisfied, and two points p_a and p_b are on different sides of the straight line $p_c p_d$, then $S = S_{acd} + S_{bcd}$.
- (5) If Condition (4) is not satisfied, and either p_c or p_d is on the straight line $p_a p_b$, then $S = |S_{acd} - S_{bcd}|$, where $| |$ is the sign of the absolute value.
- (6) If Condition (4) is not satisfied, and either p_a or p_b is on the straight line $p_c p_d$, then $S = |S_{abc} - S_{abd}|$.
- (7) If two line segments $p_a p_b$ and $p_c p_d$ are collinear, then $S = 0$.

We stipulate that the penalty cost for an unmatched line segment is the product of its length and $\frac{\sigma}{2}$, where σ is the distance threshold value given by the user.

AL, which takes advantage of the dynamic programming strategy, is formally defined as follows:

Definition 5.1. (AL): Given two compressed trajectories R' and S' with length of m and n respectively, $\Theta(R', S') =$

$$\begin{cases} \text{punish}(R') & \text{if } n = 0 \\ \text{punish}(S') & \text{if } m = 0 \\ \min \left\{ \begin{array}{l} \text{punish}(R'.r'_1) + \Theta(\text{Rest}(R'), S'), \\ \text{punish}(S'.s'_1) + \Theta(R', \text{Rest}(S')), \\ \text{dist}(R'.r'_1, S'.s'_1) + \\ \Theta(\text{Rest}(R'), \text{Rest}(S')) \end{array} \right\} & \text{otherwise} \end{cases}$$

$R'.r'_1$ and $S'.s'_1$ are the first line segments of R and S respectively. The function $\text{Rest}(T')$ return the compressed trajectory T' without its first line segment. We can easily know that $0 \leq \Theta(R', S') \leq \text{punish}(R') + \text{punish}(S') = (\text{length}(R') + \text{length}(S')) * \frac{\sigma}{2}$. If R' and S' are identical, then $\Theta(R', S') = 0$. If all pairs of line segments between R' and S' have no similarity, i.e. R' and S' are too far away from each other, then $\Theta(R', S') = \text{punish}(R') + \text{punish}(S')$. The similarity function AL is computed as below by normalizing $\Theta(R', S')$ into $[0, 1]$.

$$\begin{aligned} AL(R', S') &= 1 - \frac{\Theta(R', S')}{(\text{length}(R') + \text{length}(S')) * \frac{\sigma}{2}} \\ &= 1 - \frac{2 * \Theta(R', S')}{(\text{length}(R') + \text{length}(S')) * \sigma} \end{aligned}$$

The larger $AL(R', S')$, the greater the similarity between R' and S' is.

5.2 Top- k Similarity Query Algorithm based on AL

Definition 5.2. (Similarity Candidate Set on Compressed Trajectories): Given a compressed query trajectory T'_q , a compressed trajectory dataset \mathbb{T} and a distance threshold value σ , the similarity candidate set $\Gamma(T'_q, \sigma)$ contains all the trajectories whose minimum distance from T'_q is less than the threshold σ , i.e.,

$$\Gamma(T'_q, \sigma) = \{T' \in \mathbb{T} \mid \exists p_{i_k} p_{i_{k+1}} \in T' \text{ and } \exists p_{i_k}^q, p_{i_{k+1}}^q \in T'_q, \text{ s.t.} \\ \text{MiniDist}(p_{i_k} p_{i_{k+1}}, p_{i_k}^q, p_{i_{k+1}}^q) < \sigma\},$$

where $\text{MiniDist}()$ returns the minimum distance between two line segments.

Definition 5.3. (Top- k Similarity Query on Compressed Trajectories): Given a compressed query trajectory T'_q , a compressed trajectory dataset \mathbb{T} , a distance threshold value σ , and a positive integer k , the top- k trajectory similarity query $Q_k(T'_q, \sigma)$ returns the k most similar trajectories to T'_q in $\Gamma(T'_q, \sigma)$, satisfying: $\forall T' \in Q_k(T'_q, \sigma)$ and $\forall T'' \in (\Gamma(T'_q, \sigma) - Q_k(T'_q, \sigma))$, $AL(T', T'_q) \geq AL(T'', T'_q)$.

Due to the quadratic computation cost of AL, performing sequential scans across the entire database is not scalable. Like most trajectory similarity measures, such as LCSS, DTW, EDR and EDwP, AL and Θ are neither non-metric due to violating triangular inequality.

THEOREM 5.4. *Neither AL or Θ satisfies triangular inequality.*

PROOF. Given three compressed trajectories $T'_1 = \{(0, 0), (4, 0)\}$, $T'_2 = \{(0, 0), (4, 0), (4, 1), (7, 1)\}$, $T'_3 = \{(0, 0), (4, 0), (4, -1), (5, -1)\}$ and σ is set to 5. Then, $\Theta(T'_1, T'_2) = (1+3) * \frac{1}{2} \sigma = 10$, $\Theta(T'_1, T'_3) = (1+1) * \frac{1}{2} \sigma = 5$ and $\Theta(T'_2, T'_3) = 4$. So $\Theta(T'_1, T'_2) > \Theta(T'_1, T'_3) + \Theta(T'_2, T'_3)$. $AL(T'_1, T'_2) = \frac{1}{3}$, $AL(T'_1, T'_3) = \frac{1}{5}$ and $AL(T'_2, T'_3) = \frac{4}{35}$. So $AL(T'_1, T'_2) > AL(T'_1, T'_3) + AL(T'_2, T'_3)$. Therefore, neither AL or Θ satisfies triangular inequality. \square

Because of Theorem 5.4, generic indexing techniques, which rely on triangular inequality based pruning, can't be applied here. To speed up the query processing of $Q_k(T'_q, \sigma)$, $Q_r(R)$ is applied first to avoid unnecessary calculation in our system. This is the reason why BPA can accelerate both range queries and top- k similarity queries.

When a top- k similarity query $Q_k(T'_q, \sigma)$ is submitted to our system, the coordinates of $MBR(T'_q)$ will be calculated first. x'_{max} , x'_{min} , y'_{max} and y'_{min} are used to represent the maximum and minimum of $MBR(T'_q)$'s horizontal and vertical coordinates here. We specify a corresponding query region as R whose maximum and minimum horizontal and vertical coordinates are x_{max} , x_{min} , y_{max} and y_{min} where $x_{max} = x'_{max} + \sigma$, $x_{min} = x'_{min} - \sigma$, $y_{max} = y'_{max} + \sigma$ and $y_{min} = y'_{min} - \sigma$. Then $Q_r(R)$ is queried and we can get the result set, expressed as $\text{Result}(Q_r(R))$. $\Gamma(T'_q, \sigma)$ has been defined in Definition 5.2. We can easily get the following theorem:

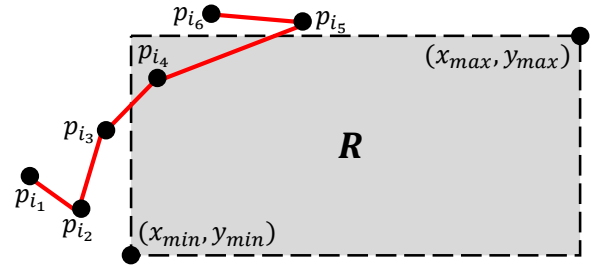


Figure 13: An example to show how to accelerate the calculation of AL.

THEOREM 5.5. *Result($Q_r(R)$) \supseteq $\Gamma(T'_q, \sigma)$. $\forall T' \in \text{Result}(Q_r(R))$, if $AL(T'_q, T') = 0$, then $T' \in \text{Result}(Q_r(R)) - \Gamma(T'_q, \sigma)$, otherwise $T' \in \Gamma(T'_q, \sigma)$.*

After that, we need to calculate the AL between T'_q and each compressed trajectory in $\text{Result}(Q_r(R))$ one by one to get the final result of $Q_k(T'_q, \sigma)$. We also propose a highly efficient acceleration strategy to speed up the calculation of AL. An example is shown in Figure 13. It's easy to know the line segments $p_{i_1}p_{i_2}$, $p_{i_2}p_{i_3}$ and $p_{i_5}p_{i_6}$ must be punished according to the definition of AL. In order to reduce the size of the two-dimensional array needed by dynamic programming and reduce the computing time of AL, these line segments can be directly punished. This is also the reason why the calculation of AL is faster than most of other trajectory similarity measures. This technique can also be applied to some other trajectory similarity measures. About how to find these line segments, we can start from the first line segment $p_{i_1}p_{i_2}$, and we can find that $p_{i_3}p_{i_4}$ is the first line segment overlapping R , so $p_{i_1}p_{i_2}$ and $p_{i_2}p_{i_3}$ can be directly punished. After that, we start from the last line segment $p_{i_5}p_{i_6}$, and we find that $p_{i_4}p_{i_5}$ is the first line segment overlapping R , so $p_{i_5}p_{i_6}$ can be directly punished. This acceleration strategy can also be used in reverse for T'_q and many line segments of T'_q can be also directly punished. In section 6.3.3, the experiment shows that this strategy can achieve up to 76.4% acceleration in average.

We should maintain a smallest heap of size k and continuously update it to get the final result set $Q_k(T'_q, \sigma)$. The number of compressed trajectories in $Q_k(T'_q, \sigma)$ may be smaller than k if there are not so many compressed trajectories similar to the queried trajectory T'_q .

6 EXPERIMENTAL EVALUATION

In this section, we compare the performance of 6 state-of-the-art trajectory compression algorithms on 3 real-life datasets which are in different motion patterns. We also evaluate the impact of different parameters on the range queries and similarity queries. All experiments are conducted on a linux machine with a 64-bit, 8-core, 3.6GHz Intel(R) Core (TM) i9-9900K CPU and 32GB memory. Our system is implemented in C++ on Ubuntu 18.04.

6.1 Datasets

Since the characteristics of GPS traces could differ substantially based on the transportation mode of moving objects, sampling rates and objects being tracked, 3 types of trajectory datasets are used

Table 2: Statistics of datasets.

	Number of Trajectories	Total Number of Points	Average Length of Trajectories (m)	Average Sampling Rate (s)	Average Distance between Two Sampling Points (m)	Total Size
Animal	327	1558407	1681350	753.009	352.872	298MB
Indoor	3578257	3634747297	43.876	0.049	0.043	224GB
Planet	8745816	2676451044	20679.7	875.015	14.6369	255GB

to examine whether a trajectory compression algorithm is robust to these differences. Statistics of these datasets are shown in Table 2. In order to reduce the I/O overhead, we artificially delete the attributes which aren't needed in the trajectories. We also remove noise before testing on these datasets.

- **Animal²**[8]: This dataset is a collection of raw trajectories to record the migration of eight young white storks originating from eight populations. This trajectories are sampled every 753s on average, and the average length between two neighbor points is 353m.
- **Indoor³**[3]: This dataset is a much larger collection of raw trajectories. It contains trajectories of visitors in the ATC shopping center in Osaka, Japan. The tracking system consists of multiple 3D range sensors, covering an area of about 900m². To capture the indoor activities more accurately, the visitor locations are sampled every 49ms on average.
- **Planet⁴**: This dataset is a very large collection of raw trajectory points. It was contributed as thousands of distinct track files by thousands of users and includes 2676451044 trajectory points in total. The sampling rates, the length of trajectories and the speeds of the tracked moving objects all vary widely.

6.2 Trajectory Compression Algorithms

There are mainly 4 ϵ -error-bounded trajectory compression algorithms in online mode, which use PED as their error metrics. They are OPW(BOPW)[15, 21], BQS[17, 18], FBQS[17, 18] and OPERB[16]. DOTS[5] has been demonstrated stable superiority against other online algorithms on many indicators[36]. Though the error metric of DOTS is not PED but LISSED, it is still put together with the other 4 algorithms to compare with ROCE. In order to provide an unbiased compression, we reimplemented all algorithms in C++, whose original languages are other than C/C++. The reimplemented code is entirely based on the original running logic, and we can get exactly the same results undergoes the strict test.

The three datasets introduced in Section 6.1 are used as the testing datasets here. We randomly sample a subset with 47 raw trajectories from Planet and a subset with 90 raw trajectories from Indoor, because some algorithms are too time-consuming to run on the entire Planet or Indoor. Some trajectories with too few points are deleted from Animal, and only 120 trajectories are left. After we delete some attributes which are not needed, the size of these three subsets are all about 57MB and we test on these three datasets in Section 6.2, except for special instructions.

²<http://dx.doi.org/10.5441/001/1.78152p3q>

³https://irc.atr.jp/crest2010_HRI/ATC_dataset/

⁴<https://wiki.openstreetmap.org/wiki/Planet.gpx>

6.2.1 Compression Time. In the first experiment, we evaluate the compression time of 6 compression algorithms w.r.t. varying the average compression rate, and the results are shown in Figure 14. For fairness, we load and compress trajectories one by one, and only count the run time of the compressing process. FBQS is a little faster than BQS, because FBQS doesn't perform complex calculations, but the price is the tolerable loss of the average compression rate. BQS and FBQS are the slowest algorithms when the average compression rate is low. As the average compression rate gets higher, the execution time needed by DOTS increases rapidly, and DOTS becomes the slowest algorithm. In the third subimage of Figure 14, the execution time of DOTS is far more than other algorithms when the average compression rate is more than 100. So we stop doing the experiment. For DOTS, it does badly in the situations where the tracked object stays at the same place for a long time, and it needs much more memory and time to handle this kind of situations. The subset of Planet has some such trajectories, and this is the reason why DOTS is so time-consuming on the subset of Planet. OPERB, OPW and ROCE are always the fastest algorithms, and they are all fast enough to compress trajectories.

6.2.2 Accuracy Loss. In order to show the the accuracy loss of these 6 algorithms, we evaluate the maximum PSED error of compressed trajectories compressed by these 6 compression algorithms w.r.t. varying the average compression rate, and the results are shown in Figure 15. In the first and the second subimage, the maximum PSED errors of DOTS, OPERB and OPW are much bigger than ROCE, FBQS and BQS. In the third subimage, OPERB and OPW do badly in the maximum PSED errors. We also evaluate the average PSED error of compressed trajectories compressed by these 6 compression algorithms w.r.t. varying the average compression rate, and the results are shown in Figure 16. ROCE always performs better than most of other algorithms. In summary, ROCE maintains less accuracy loss.

6.2.3 Trajectory Point Number. To evaluate the impact of data point number in trajectories, we fix the average compression rates of these 3 testing datasets as 50 and vary the point number of every trajectory from 10% to 100% of the raw trajectory. Suppose one raw trajectory has 10000 points and we reduce the number of trajectory points to 20%, then we randomly sample a trajectory segment with 2000 continuous trajectory points from the raw trajectory, instead of randomly sampling 2000 trajectory points. We can see the changes in compression time of different algorithms in Figure 17. Only ROCE and OPERB always perform well in these three datasets. The rates of ROCE and OPERB are always around 10 when the point number of these trajectories become tenfold. Other algorithms all need much more time to compress longer trajectories. In other words, only ROCE and OPERB are suitable to compress extremely long trajectories.

6.2.4 Compression Delay. For all algorithms in batch mode, only all points of a raw trajectory have been loaded and then we can get the first compressed point (or line segment). So the compression delays of algorithms in batch mode are all very high. As for all algorithms in online mode, such as these 6 algorithms, the compressed points (or line segments) are output continuously as the raw trajectory points being input to it one by one. So the compression delays

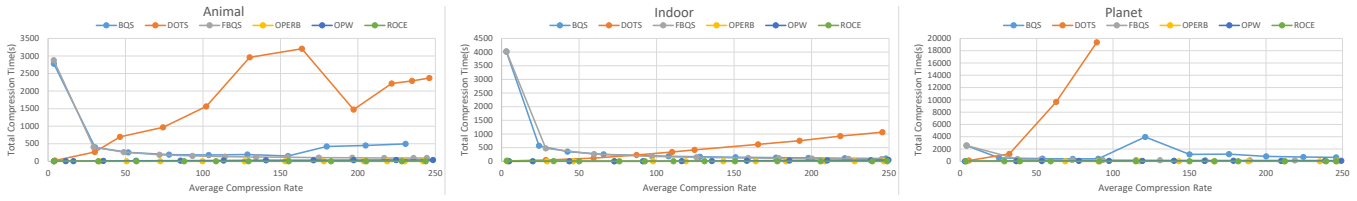


Figure 14: The total compression time of 6 compression algorithms.

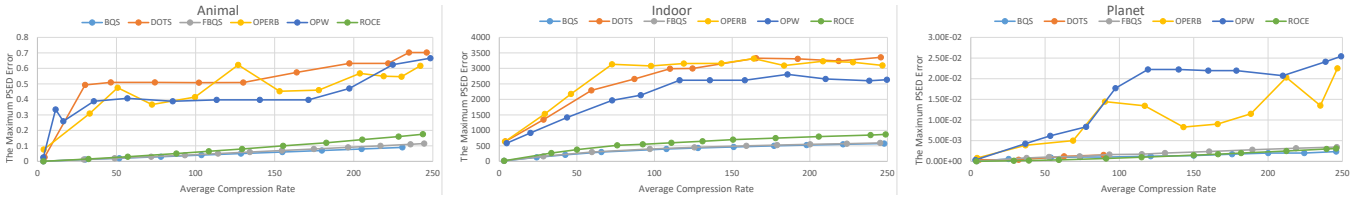


Figure 15: The maximum PSED error of 6 compression algorithms.

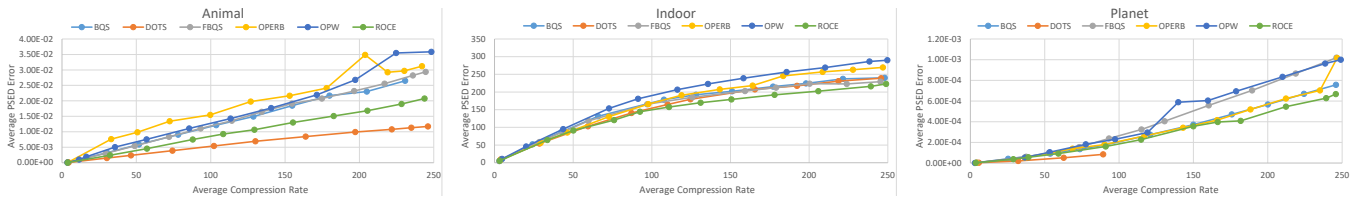


Figure 16: The average PSED error of 6 compression algorithms.

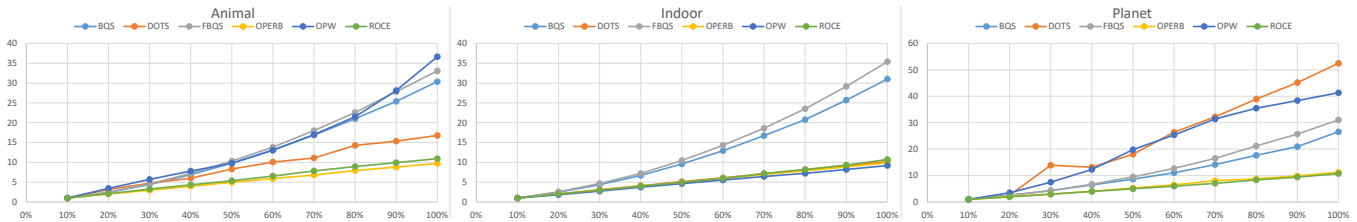


Figure 17: The x-coordinate is the rate of the sampled trajectory point number to the raw trajectory point number. The y-coordinate is the rate of compression time for the sampled trajectories to the compression time for 10% sampled trajectories.

of these algorithms are relatively low. These 6 algorithms all have uncertain delays. The uncertainty is introduced by the uncertain entered data and different compression process. We evaluate the delays of these 6 algorithms on three long trajectories from Animal, Indoor and Planet, whose point numbers are 75000, 350000 and 80000 respectively. The compression rates for all trajectories and algorithms are all fixed as 100. The results are shown in Figure 18. We can see that only the average delay of DOTS is always the highest because of an incremental directed acyclic graph construction. The delays of all the other algorithms are relatively low.

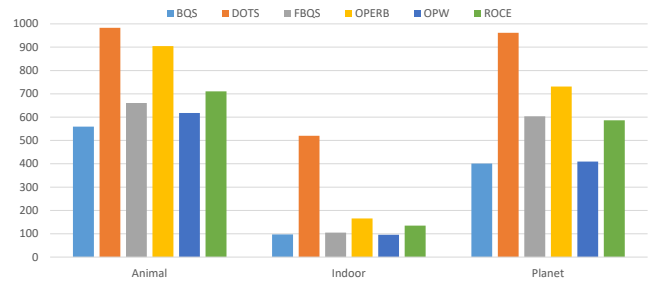


Figure 18: The average delays of 6 algorithms on 3 long trajectories.

6.2.5 *Compressed Trajectories in Actual Use.* In order to evaluate the deviation between the compressed trajectories compressed by different compression algorithms and the raw trajectories in actual use, let's define the evaluation metrics first. Given a range query, let

Q_R denote the trajectories returned from the raw trajectory database and Q_C denote the trajectories returned from the compressed

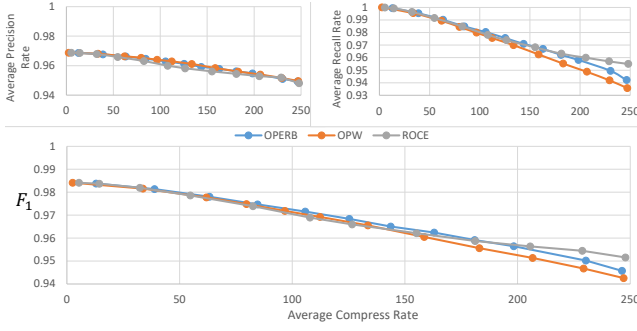


Figure 19: The comparison of the average precision rates and recall rates of range queries on the compressed trajectories compressed by three fast compression algorithms.

database. Similar to most related work, when we want to get Q_R , the range queries on the raw dataset are all based on points and the results are identified as the right results. For Q_C , the range queries on the compressed dataset are all based on segments. The precision rate P of a range query is defined as

$$P = \frac{|Q_R \cap Q_C|}{|Q_C|}$$

The recall rate R is defined as

$$R = \frac{|Q_R \cap Q_C|}{|Q_R|}$$

For comprehensive comparison of P and R , F_1 -Measure, which is the harmonic mean of P and R , is defined as

$$\frac{1}{F_1} = \frac{1}{2} * \left(\frac{1}{P} + \frac{1}{R} \right)$$

In this experiment, we use a subset of Planet as our testing dataset. We select all trajectories with a dimension of time and completely within the rectangular region which is from 7 degrees east longitude to 14 degrees east longitude and from 46 degrees north latitude to 53 degrees north latitude, because it's one of the regions which have the densest trajectories. With a total size of 2.3GB, this subset has 22974 trajectories. We only choose OPERB, OPW and ROCE as the testing algorithms, because BQS, DOTS and FBQS are all too time consuming to compress such a big dataset. 100000 squares for range queries, whose area are all $5km^2$, are randomly generated and fixed. Then we evaluate the average precision and recall w.r.t. varying the average compression rate, and the results are shown in Figure 19. We can see that range queries based on segments on the compressed trajectories all perform very well, no matter which kind of compression algorithms is used. The average precisions of these 3 algorithms are almost exactly the same. On the average recall rate, although the average recall rates of these 3 algorithms are all high enough, ROCE performs a little better than OPERB and OPW. Thus, on the average F_1 , ROCE is still the best of these 3 algorithms. In short, ROCE performs better than other algorithms in actual use.

6.3 Query on Compressed Trajectories

In this part, from Planet, we select all trajectories completely within a rectangular region, the same with the region in Section 6.2.5, as

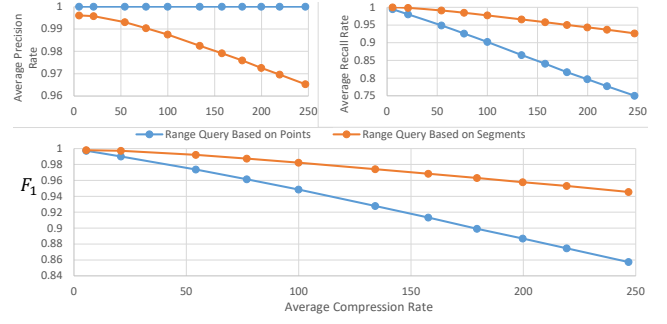


Figure 20: The comparison of the average precision rates and recall rates of range queries based on points and segments.

our testing dataset. Every trajectory point only has been left only two attributes, i.e. longitude and latitude. Then, we can get a subset with 96279 raw trajectories and a total size of 6.8GB. Except for special instructions, the following experiments are all performed on this subset or its compressed forms which are compressed by ROCE.

6.3.1 Range Query based on Segments. Each time, we run 100000 range queries generated randomly, whose areas are all $16km^2$, on this subset for testing or its corresponding compressed forms. Figure 20 shows the average precision rates P s and recall rates R s of range queries based on points and segments. P and R are calculated by the difference between the results of range queries on the raw dataset and compressed datasets. Similar to most related work, the range queries on the raw dataset are all based on points, and the results are identified as the standard results. The P s of range queries based on points are always equal to 1 because the points of a compressed trajectory is a subset of the corresponding raw trajectory points. But as the average compression rate increases, R of range queries based on points declines sharply. This means that range queries on the compressed dataset based on points leave up to nearly 25% trajectories undiscovered, whose corresponding raw trajectories overlap the query regions. But range queries based on segments do much better than range queries based on points. As the average compression rate increases, though P of range queries based on segments drops a little, the R of range queries based on segments is much higher than the one of range queries based on points. For comprehensive comparison of P and R , we also compare the value of F_1 . The F_1 of range queries based on segments can be up to 10.3% more than the ones based on points. So it's more suitable to execute range queries on the compressed trajectories based on segments.

Then, we compare the time of range queries on the raw trajectories based on points and the one of range queries on the compressed trajectories based on segments. For fairness, we don't use any index to accelerate range queries with points or segments. Randomly generated 10000 range queries are executed every time. The results are shown in Figure 21. We can see that range queries on the compressed trajectories with segments need much less time than range queries on the raw trajectories with points. As the average compression rate increases, range queries on the compressed trajectories with segments need less time. So it's very efficient and

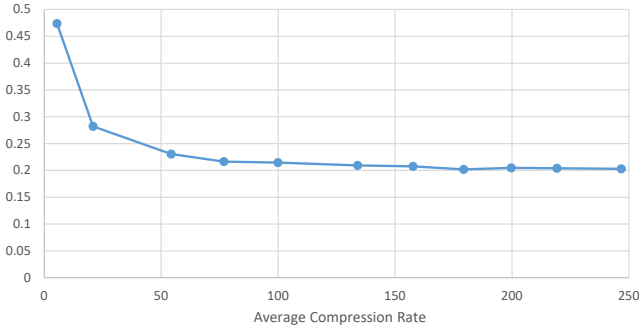


Figure 21: The y-coordinate is the rate of the execution time needed by range queries on the compressed trajectories with segments to the execution time needed by range queries on the raw trajectories with points.

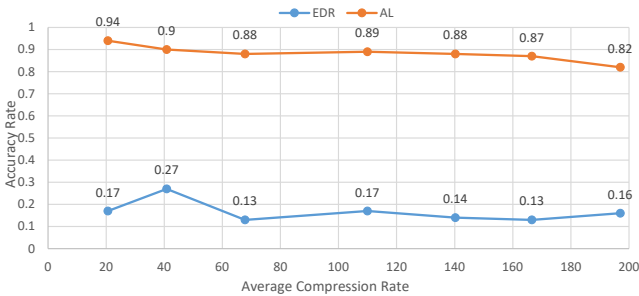


Figure 22: Comparison of EDR and AL on compressed trajectories.

suitable to execute range queries on the compressed trajectories based on segments.

6.3.2 Trajectory Error-based Quality Metric Based on Point or Segment. We randomly select a raw trajectory from Planet, and then 5472 raw trajectories similar to the chosen trajectory are selected to form a testing dataset. The total size of this testing dataset is 502.9MB and each trajectory point has only two dimensions, latitude and longitude. Then, this testing dataset is compressed by ROCE into compressed datasets with different average compression rates. We choose EDR as the trajectory error-based quality metric based on point to compare with AL, because EDR is more robust and accurate than other distance functions[6, 35]. If a trajectory error-based quality metric is suitable for the compressed trajectories, there should be only a few differences between the results of similarity queries on compressed trajectories with different average compression rates. So we set the result of top-100 similarity query on the compressed trajectories, whose average compression rate are 3.607817, as the standard result for EDR and AL respectively. Then we change the average compression rate to see the changes in accuracy rate. The results are shown in Figure 22. The accuracy rates of AL are all much higher than the ones of EDR, and it's quite obvious that AL is much more suitable for similarity queries on compressed trajectories.

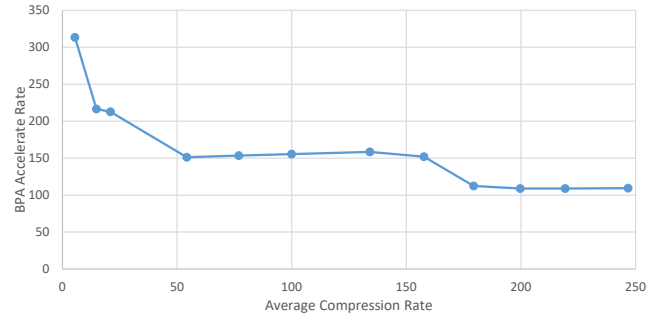


Figure 23: The accelerate rate obtained by using BPA.

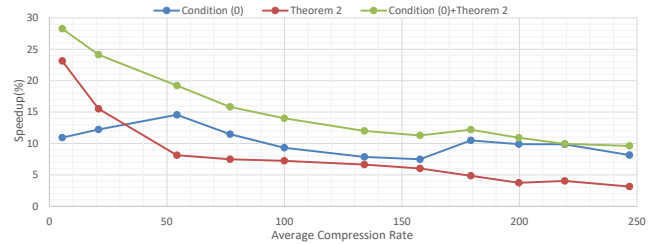


Figure 24: The speedup of Condition (0) and Theorem 4.4.

6.3.3 Speedup Strategies. In this part, we will show how much acceleration rate can be obtained by using BPA. Randomly generated 10000 range queries generated are run on the compressed trajectories with different average compression rates. The areas of the query regions are all $16km^2$. The results are shown in Figure 23. It's quite obvious that BPA can accelerate range queries greatly. By using BPA, we can reduce the query time to at least $1/109$. BPA can accelerate the range queries much more obviously when the average compression rate of the compressed trajectories gets smaller.

Then, we test how much acceleration can be obtained by Condition (0) and Theorem 4.4 in Section 4.1. We change the average compression rate and run 10000 randomly generated range queries each time. The results are shown in Figure 24. The average accelerations of Condition (0) and Theorem 4.4 respectively are 10.21% and 8.18%. When both of them are used, the average acceleration is 15.23%. The acceleration is much more effective when the average compression rate gets lower.

Last, we want to show how much acceleration can be obtained by the acceleration technique for AL exemplified with Figure 13. σ is set to 0.01 in longitude and latitude (about $0.7 \sim 1.1km$). Ten similarity queries are generated randomly and we vary the value of the average compression rate to see the changes in the acceleration which can be obtained by this acceleration technique. The results are shown in Figure 25. From the results of the experiment, the speedup is quite satisfactory and the average speedup value is up to 77.5%. Another advantage of this acceleration technique is that the acceleration is not much sensitive to the value of the average compression rate.

6.3.4 Effect of ξ . ξ controls whether one node in BPA is a father node of four child nodes or a leaf node. In this experiment, we

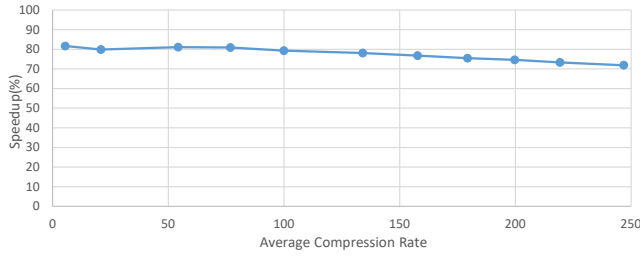


Figure 25: The speedup of the acceleration technique for AL exemplified with Figure 13.

Table 3: ξ has impact on the average height of BPA and the total range query time.

ξ	1000	2000	4000	8000	16000	32000	64000
Average Height	9.63914	8.54705	7.35638	6.11496	5.08759	5	4
Total Range Query Time(s)	3.48211	3.4858	5.38222	5.32648	9.92246	10.0195	21.8855

evaluate the average height of BPA and the execution time of the range queries on the compressed trajectories w.r.t. varying ξ . The average height of BPA is defined as the average height of all leaf nodes and the height of the root node is 1. We fix the average compression rate of the compressed trajectories as 100 and run 100000 range queries generated randomly, whose areas are all $16km^2$. The statistical results of this experiment are shown in Table 3. It can be seen that ξ controls the average height of BPA. The average height has impact on the time needed by range queries. The greater the average height of BPA is, the less time is needed by range queries. The heights of all leaf nodes are almost the same. Especially when $\xi = 32000$ or $\xi = 64000$, the heights of all leaf nodes are all the same, which probes that BPA is well balanced and our node partitioning strategy dose work. ξ is always fixed as 2000 in other experiments.

6.3.5 Effect of Query Region. In this experiment, we verify the impact of the area of the query region on the query result and the execution time. The average compression rate of the compressed trajectories is fixed as 100. We change the area of the query regions and run 100000 randomly generated range queries each time. The results are shown in Figure 26 and Figure 27. We can see that the average trajectories number in the result of a single range query and the total execution time of 100000 range queries grows approximately linearly with the area of the query regions. From the results in Figure 26, our system is quite efficient and able to support about than 30000 range queries in just one second.

6.3.6 Effect of σ . σ determines the minimum distance beyond which two line segments or trajectories are considered to have no similarities. We study the effect of σ on the total number of calculation times of AL in a single top- k similarity query on the compressed trajectories. The bigger σ , the larger query regions we will use to execute trajectory range queries before we execute the calculations of AL. In this experiment, we fix the average compression rate as 100, and 10 randomly generated similarity queries are executed each time. The results are shown in Figure 28 and Figure 29. The average execution time and the average calculation times

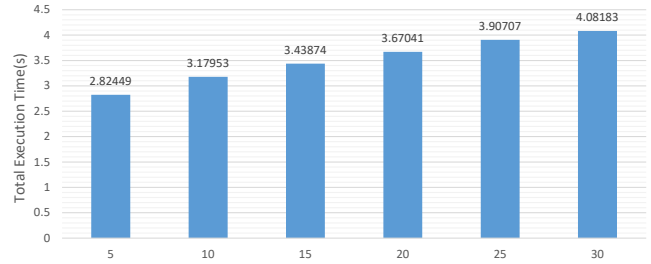


Figure 26: The variation in the total execution time of 100000 range query. The x-coordinate is the area of each query region and in km^2 .

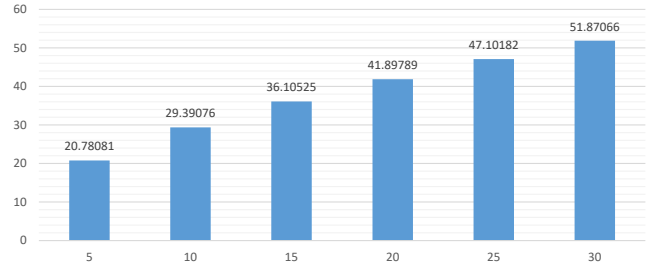


Figure 27: The variation in the average number of trajectories in the result of a single range query. The x-coordinate is the area of each query region and in km^2 .

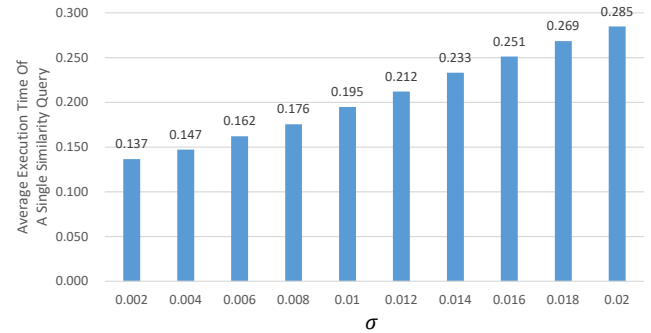


Figure 28: The average execution time of a single top- k similarity query. σ is in longitude and latitude.

of AL in a single top- k similarity query both grow when σ gets larger. The increase in the calculation times of AL dose influence the execution time of similarity queries, but it's only part of the reason. The other main reason is that the calculation of each AL is also more time-consuming, because more pairs of line segments are thought to have a certain similarity and more areas sandwiched by pairs of line segments need to be calculated.

7 RELATED WORK

Compression algorithms in online mode. With much more application scenarios compared with algorithms in batch mode, trajectory compression algorithms in online mode attract people's attention and some algorithms have been proposed based on different

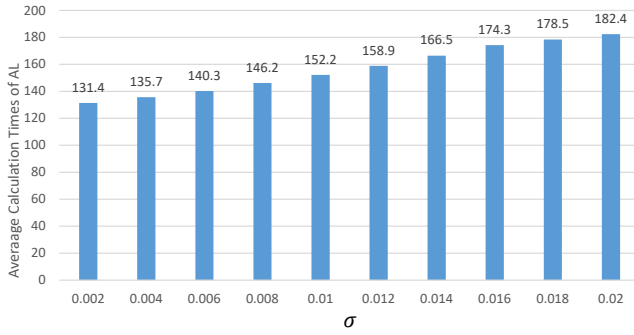


Figure 29: The average calculation times of AL in a single top- k similarity query. σ is in longitude and latitude.

error criterions. There are mainly 4 frequently-used error criterions, i.e. PED, SED, DAD and LISSED, which are adopted to define the distance between a raw trajectory point and its corresponding line segment after the compression. Among them, DAD(Angular[13], Interval[12]) defines the distance based on the greatest angular difference between two directions. DAD doesn't take into account the Euclidean distance between each trajectory point and its corresponding line segment after the compression, a key weakness of DAD is that a raw trajectory point may be too far away from its corresponding line segment after the compression and this line segment can't represent such a raw trajectory point well. SED(OPW-TR[21], STTrace[26], SQUISH[23], SQUISH-E(λ)[24], SQUISH-E(μ)[24]) and LISSED(DOTS[5]) use the attribute of time to find the corresponding synchronized point of each raw trajectory point on its corresponding line segment, then SED and LISSED are calculated based on the Euclidean distance between the raw point and its corresponding synchronized point. But the utilities of SED and LISSED are limited because the time attribute isn't always available because of privacy or other reasons. Have been introduced in Section 3.1, PED(OPW[15, 21], BQS[17, 18], FBQS[17, 18], OPERB[16]) can be used in more application scenarios than SED and LISSED. OPW was put forward very early. It starts from the first trajectory point and compresses as more points as possible into a line segment until the maximum error exceeds the predefined threshold. It will repeat this processing procedure until the entire trajectory has been compressed. BQS is also an ϵ -error-bounded trajectory compression algorithm. It builds a virtual coordinate system centered at the starting point. In each of 4 quadrants, it picks at most eight important points to form a convex hull which encloses all points in this quadrant. Then in each quadrant, an upper bound and a lower bound are calculated so that in most cases, a point can be quickly decided for removal or preservation without expensive error calculation. Only in a few cases, complicated error calculation are needed. FBQS is the fast version of BQS. In FBQS, error calculations are no longer needed, and a raw trajectory point is directly reserved if it needs error calculation in BQS. Such a strategy make FBQS get lower compression rate with the same error bounded error, though FBQS is a little faster. Based on a novel local distance checking method, OPERB uses a directed line segment to approximate the buffered points. Several optimization techniques are used to improve the compression rate. Though OPERB is very fast because it does only

a few calculations, the quantity of accuracy loss is too much. The detailed comparisons of these 4 algorithm and ROCE have been shown in Section 6.2

Semantic trajectory compression. Semantic trajectory compression[4, 14, 19, 29, 33] is a kind of lossy trajectory compression techniques. Semantic trajectory compression assumes that the objects being tracked are moving along with road networks and tries to map all GPS points to continuous road segments with map matching algorithms[2, 11, 20, 25, 31, 34, 37] by making use of the knowledge of the road networks. Various queries can be executed on the result of the semantic trajectory compression. Though semantic trajectory compression algorithms can get a high compression rate, they still have two main weaknesses which limit their application. First, they require additional and detailed road network information, but many trajectories such as migrations of animals, the indoor movements and the movements of ships or airplanes, are not constrained within road networks. Second, it has been shown that map matching algorithms are not accurate if the trajectory sampling rate is low. These methods and line simplification based methods are orthogonal to each other, and may be combined with each other to further improve the effectiveness of trajectory compression.

Trajectory Similarity Measures. Trajectories, whose data points are in the form of GPS points, are a special form of time series. Most of widely used measures, which evaluate the similarity between time series, only focus on the distances between matched point pairs of different time series, such as Euclidean distance (ED)[7, 32], Dynamic Time Warping (DTW)[1], the Longest Common Subsequence (LCSS)[30], Edit Distance on Real sequences (EDR)[6], Sequence Weighted Alignment model (Swale)[22], Model-driven Assignment (MA)[28] and so on.

For the sake of illustration, let R and S be two time series with length of m and n respectively, and r_i and s_j be the points in time series R and S respectively. Each point of R and S is expressed as $(r_{i,x}, r_{i,y}, r_{i,t})$ and $(s_{j,x}, s_{j,y}, s_{j,t})$ respectively. The most straightforward similarity measure for time series is the Euclidean Distance. It requires that both time series have the same number of points and calculates the Euclidean distance between each pair of points in each time series i.e.

$$ED(R, S) = \sqrt{\sum_{i=1}^n (r_{i,x} - s_{i,x})^2 + (r_{i,y} - s_{i,y})^2}.$$

Dynamic programming is adopted in more complicated similarity measures, including DTW, LCSS, EDR and Swale. These 4 measures are summarized in Table 4. $Rest(R)$ and $Rest(S)$ denote R and S without the first point respectively. $dist(r_i, s_j) = L_2$ norm. In the definition of EDR, if $(|r_{1,x} - s_{1,x}| \leq \epsilon) \wedge (|r_{1,y} - s_{1,y}| \leq \epsilon)$ can be satisfied, $subcost = 0$, else $subcost = 1$. As for the definition of Swale, let the gap cost (i.e. the mismatch penalty) be gap_c and the match reward be $reward_m$. These two values require users or domain experts with the particular knowledge of a certain area to tune for optimal performance. MA uses a directed graph whose edges are bidirectional to show two points of different trajectories can be matched or not, which makes MA more flexible in aligning points of two trajectories. However, it has been proved that MA is not reasonable enough in some cases[27]. Though DTW, LCSS,

Table 4: Definitions of 4 trajectory error-based quality metrics.

	Definition
$DTW(R, S) =$	$\begin{cases} 0 & \text{if } m = n = 0 \\ \infty & \text{if } m = 0 \text{ or } n = 0 \\ \text{dist}(r_1, s_1) + \min \begin{cases} DTW(Rest(R), Rest(S)), \\ DTW(Rest(R), S), \\ DTW(R, Rest(S)) \end{cases} & \text{otherwise} \end{cases}$
$LCSS(R, S) =$	$\begin{cases} 0 & \text{if } m = 0 \text{ or } n = 0 \\ 1 + LCSS(Rest(R), Rest(S)) & \text{if } \forall d, r_{d,1} - s_{d,1} \leq \epsilon \\ \max \{ LCSS(Rest(R), S), \\ LCSS(R, Rest(S)) \} & \text{otherwise} \end{cases}$
$EDR(R, S) =$	$\begin{cases} n & \text{if } m = 0 \\ m & \text{if } n = 0 \\ \min \begin{cases} \text{subcost} + EDR(Rest(R), Rest(S)), \\ 1 + EDR(Rest(R), S), \\ 1 + EDR(R, Rest(S)) \end{cases} & \text{otherwise} \end{cases}$
$Swale(R, S) =$	$\begin{cases} n * gap_c & \text{if } m = 0 \\ m * gap_c & \text{if } n = 0 \\ \text{reward}_m + Swale(Rest(R), Rest(S)) & \text{if } \forall d \in \{x, y\}, r_{1,d} - s_{1,d} \leq \epsilon \\ \max \{ gap_c + Swale(Rest(R), S), \\ gap_c + Swale(R, Rest(S)) \} & \text{otherwise} \end{cases}$

EDR, Swale and MA are extensively used, none of them are suitable for compressed trajectories as discussed in Section 5.1. From another viewpoint of integral, DISSIM[9] defines the spatiotemporal dissimilarity between two trajectories R and S during a definite time interval $[t_1, t_n]$ by integrating their Euclidean distance in time. DISSIM is defined as follows:

$$DISSIM(R, S) = \int_{t_1}^{t_n} D_{R,S}(t) dt,$$

where $D_{R,S}(t)$ is the function of the Euclidean distance between trajectories R and S with time. One of DISSIM's shortcomings can be obviously found out from its definition. DISSIM thinks highly of the time dimension when measuring the distance between two trajectories. This means two trajectories must have not only similar shapes, but also similar speeds if they are determined to be similar. While in practical applications, it's not a must. Edit Distance with Projections (EDwP)[27] is designed for raw trajectories under inconsistent and variable sampling rates. First, EDwP connects each two adjacent trajectory sampling points with a line segment. EDwP may cut each line segment into at most two line segments. After that, EDwP uses a measure, like area but not area, to calculate the distance between each pair of line segments. Then, the minimum sum of such calculations is the final result of EDwP between two raw trajectories. Different from EDWP, for AL, the calculation of the distance between each pair of line segments is really the area sandwiched by these two line segments under any condition.

8 CONCLUSIONS

In this paper, in consideration of that the compressed trajectories should be composed with continuous line segments rather than discrete trajectory points, we come up with a whole set of complete solutions for efficient queries on compressed trajectories, including the trajectory compression algorithm ROCE which is error bounded, range queries and top- k similarity queries on compressed trajectories composed of consecutive line segments. We are the first to revise PED error criterion and propose a more reasonable error criterion PSED. In terms of top- k similarity queries on compressed

trajectories, we use the feature of two continuous line segments to define a new trajectory error-based quality metric AL. An efficient trajectory index tree BPA is also proposed to speed up range queries and top- k similarity queries obviously. A lot of small but effective techniques are also used to avoid unnecessary complex calculation.

REFERENCES

- [1] Donald J Berndt and James Clifford. 1994. Using dynamic time warping to find patterns in time series. In *KDD workshop*, Vol. 10. Seattle, WA, 359–370.
- [2] Sotiris Brakatsoulas, Dieter Pfoser, Randall Salas, and Carola Wenk. 2005. On map-matching vehicle tracking data. In *Proceedings of the 31st international conference on Very large data bases*. VLDB Endowment, 853–864.
- [3] Dražen Brščić, Takayuki Kanda, Tetsushi Ikeda, and Takahiro Miyashita. 2013. Person tracking in large public spaces using 3-D range sensors. *IEEE Transactions on Human-Machine Systems* 43, 6 (2013), 522–534.
- [4] Hu Cao and Ouri Wolfson. 2005. Nonmaterialized motion information in transport networks. In *International Conference on Database Theory*. Springer, 173–188.
- [5] Weiquan Cao and Yunzhao Li. 2017. DOTS: An online and near-optimal trajectory simplification algorithm. *Journal of Systems and Software* 126 (2017), 34–44.
- [6] Lei Chen, M Tamer Özsu, and Vincent Oria. 2005. Robust and fast similarity search for moving object trajectories. In *Proceedings of the 2005 ACM SIGMOD international conference on Management of data*. ACM, 491–502.
- [7] Christos Faloutsos, M. Ranganathan, and Yannis Manolopoulos. 1994. Fast Subsequence Matching in Time-Series Databases. In *Proceedings of the 1994 ACM SIGMOD International Conference on Management of Data* (Minneapolis, Minnesota, USA) (*SIGMOD '94*). Association for Computing Machinery, New York, NY, USA, 419–429. <https://doi.org/10.1145/191839.191925>
- [8] A Flack, W Fiedler, J Blas, I Pokrovski, B Mitropolsky, M Kaatz, K Aghababayan, A Khachatryan, I Fakriadis, E Makrigianni, L Jerzak, M Shamin, C Shamina, H Azafzaf, C Feltrup-Azafzaf, TM Mokotjomela, and M Wikelski. 2015. Data from: Costs of migratory decisions: a comparison across eight white stork populations. <https://doi.org/doi:10.5441/001/1.78152p3q>
- [9] Elias Frenzos, Kostas Gratsias, and Yannis Theodoridis. 2007. Index-based Most Similar Trajectory Search. In *IEEE International Conference on Data Engineering*.
- [10] John Edward Hershberger and Jack Snoeyink. 1992. *Speeding up the Douglas-Peucker line-simplification algorithm*. University of British Columbia, Department of Computer Science.
- [11] Gang Hu, Jie Shao, Fenglin Liu, Yuan Wang, and Heng Tao Shen. 2017. IF-matching: towards accurate map-matching with information fusion. *IEEE Transactions on Knowledge and Data Engineering* 29, 1 (2017), 114–127.
- [12] Bingqing Ke, Jie Shao, and Dongxiang Zhang. 2017. An efficient online approach for direction-preserving trajectory simplification with interval bounds. In *2017 18th IEEE International Conference on Mobile Data Management (MDM)*. IEEE, 50–55.
- [13] Bingqing Ke, Jie Shao, Yi Zhang, Dongxiang Zhang, and Yang Yang. 2016. An online approach for direction-based trajectory compression with error bound guarantee. In *Asia-Pacific Web Conference*. Springer, 79–91.
- [14] Georgios Kellaris, Nikos Pelekis, and Yannis Theodoridis. 2013. Map-matched trajectory compression. *Journal of Systems and Software* 86, 6 (2013), 1566–1579.
- [15] Eamonn Keogh, Selina Chu, David Hart, and Michael Pazzani. 2001. An online algorithm for segmenting time series. In *Proceedings 2001 IEEE International Conference on Data Mining*. IEEE, 289–296.
- [16] Xuelian Lin, Shuai Ma, Han Zhang, Tianyu Wo, and Jinpeng Huai. 2017. One-pass error bounded trajectory simplification. *Proceedings of the VLDB Endowment* 10, 7 (2017), 841–852.
- [17] Jiajun Liu, Kun Zhao, Philipp Sommer, Shuo Shang, Brano Kusy, and Raja Jurdak. 2015. Bounded quadrant system: Error-bounded trajectory compression on the go. In *2015 IEEE 31st International Conference on Data Engineering*. IEEE, 987–998.
- [18] Jiajun Liu, Kun Zhao, Philipp Sommer, Shuo Shang, Brano Kusy, Jae-Gil Lee, and Raja Jurdak. 2016. A novel framework for online amnesic trajectory compression in resource-constrained environments. *IEEE Transactions on Knowledge and Data Engineering* 28, 11 (2016), 2827–2841.
- [19] Kuilen Liu, Yaguang Li, Jian Dai, Shuo Shang, and Kai Zheng. 2014. Compressing large scale urban trajectory data. In *Proceedings of the Fourth International Workshop on Cloud Data and Platforms*. ACM, 3.
- [20] Yin Lou, Chengyang Zhang, Yu Zheng, Xing Xie, Wei Wang, and Yan Huang. 2009. Map-matching for low-sampling-rate GPS trajectories. In *Proceedings of the 17th ACM SIGSPATIAL international conference on advances in geographic information systems*. ACM, 352–361.
- [21] Nirvana Meratnia and A Rolf. 2004. Spatiotemporal compression techniques for moving point objects. In *International Conference on Extending Database Technology*. Springer, 765–782.
- [22] Michael D Morse and Jignesh M Patel. 2007. An efficient and accurate method for evaluating time series similarity. In *Proceedings of the 2007 ACM SIGMOD international conference on Management of data*. ACM, 569–580.

- [23] Jonathan Muckell, Jeong-Hyon Hwang, Vikram Patil, Catherine T Lawson, Fan Ping, and SS Ravi. 2011. SQUISH: an online approach for GPS trajectory compression. In *Proceedings of the 2nd International Conference on Computing for Geospatial Research & Applications*. ACM, 13.
- [24] Jonathan Muckell, Paul W Olsen, Jeong-Hyon Hwang, Catherine T Lawson, and SS Ravi. 2014. Compression of trajectory data: a comprehensive evaluation and new approach. *Geoinformatica* 18, 3 (2014), 435–460.
- [25] Paul Newson and John Krumm. 2009. Hidden Markov map matching through noise and sparseness. In *Proceedings of the 17th ACM SIGSPATIAL international conference on advances in geographic information systems*. ACM, 336–343.
- [26] Michalis Potamias, Kostas Patrourmpas, and Timos Sellis. 2006. Sampling trajectory streams with spatiotemporal criteria. In *18th International Conference on Scientific and Statistical Database Management (SSDBM'06)*. IEEE, 275–284.
- [27] Sayan Ranu, P Deepak, Aditya D Telang, Prasad Deshpande, and Sriram Raghavan. 2015. Indexing and matching trajectories under inconsistent sampling rates. In *2015 IEEE 31st International Conference on Data Engineering*. IEEE, 999–1010.
- [28] Swaminathan Sankararaman, Pankaj K Agarwal, Thomas Mølhave, Jiangwei Pan, and Arnold P Boedihardjo. 2013. Model-driven matching and segmentation of trajectories. In *Proceedings of the 21st ACM SIGSPATIAL International Conference on Advances in Geographic Information Systems*. ACM, 234–243.
- [29] Renchu Song, Weiwei Sun, Baihua Zheng, and Yu Zheng. 2014. PRESS: A novel framework of trajectory compression in road networks. *Proceedings of the VLDB Endowment* 7, 9 (2014), 661–672.
- [30] Michail VLACHOS, George KOLLIOS, and Dimitrios GUNOPULOS. 2002. Discovering similar multidimensional trajectories. In *International conference on data engineering*. 673–684.
- [31] Carola Wenk, Randall Salas, and Dieter Pfoser. 2006. Addressing the need for map-matching speed: Localizing global curve-matching algorithms. In *18th International Conference on Scientific and Statistical Database Management (SSDBM'06)*. IEEE, 379–388.
- [32] Byoung-Kee Yi and Christos Faloutsos. 2000. Fast time sequence indexing for arbitrary Lp norms. In *VLDB*, Vol. 385. 99.
- [33] Haitao Yuan and Guoliang Li. 2019. Distributed In-Memory Trajectory Similarity Search and Join on Road Network. In *2019 IEEE 35th International Conference on Data Engineering (ICDE)*. IEEE, 1262–1273.
- [34] Jing Yuan, Yu Zheng, Chengyang Zhang, Xing Xie, and Guang-Zhong Sun. 2010. An interactive-voting based map matching algorithm. In *Proceedings of the 2010 Eleventh International Conference on Mobile Data Management*. IEEE Computer Society, 43–52.
- [35] Bowen Zhang, Yanyan Shen, Yanmin Zhu, and Jiadi Yu. 2018. A GPU-accelerated framework for processing trajectory queries. In *2018 IEEE 34th International Conference on Data Engineering (ICDE)*. IEEE, 1037–1048.
- [36] Dongxiang Zhang, Mengting Ding, Dingyu Yang, Yi Liu, Ju Fan, and Heng Tao Shen. 2018. Trajectory Simplification: An Experimental Study and Quality Analysis. *Proc. VLDB Endow.* 11, 9 (May 2018), 934–946. <https://doi.org/10.14778/3213880.3213885>
- [37] Dongxiang Zhang, Dingyu Yang, Yuan Wang, Kian-Lee Tan, Jian Cao, and Heng Tao Shen. 2017. Distributed shortest path query processing on dynamic road networks. *The VLDB Journal—The International Journal on Very Large Data Bases* 26, 3 (2017), 399–419.